

# Real-time measurements of NMVOCs in the central IGB, Lucknow, India: Source characterization and their role in O<sub>3</sub> and SOA formation

Formatted: Left: 2.54 cm, Right: 2.54 cm, Top: 2.54 cm, Bottom: 2.54 cm, Numbering: Continuous

Vaishali Jain<sup>1</sup>, Nidhi Tripathi<sup>3</sup>, Sachchida N. Tripathi<sup>1,2</sup>, Nidhi Tripathi<sup>3</sup>, Mansi Gupta<sup>3</sup>, Lokesh K. Sahu<sup>3</sup>, Vishnu Murari<sup>1</sup>, Sreenivas Gaddamidi<sup>1</sup>, Ashutosh K. Shukla<sup>1</sup>, Andre S.H. Prevot<sup>4</sup>

<sup>1</sup>Department of Civil Engineering, Indian Institute of Technology Kanpur, Kanpur, 208016, India

<sup>2</sup>Centre for Environmental Science and Engineering, Indian Institute of Technology Kanpur, Kanpur, 208016, India

<sup>3</sup>Space and Atmospheric Sciences Division, Physical Research Laboratory, Ahmedabad, 380009, India

<sup>4</sup>Laboratory of Atmospheric Chemistry, Paul Scherrer Institute, 5232, Switzerland

Correspondence to: Dr Sachchida N. Tripathi ([snt@iitk.ac.in](mailto:snt@iitk.ac.in)), Dr. Lokesh K. Sahu ([Lokesh@prl.res.in](mailto:Lokesh@prl.res.in))

**Abstract:** Lucknow is the capital of India's largest state, Uttar Pradesh, one of South Asia's most polluted urban cities. Tropospheric photochemistry relies on non-methane volatile organic compounds (NMVOCs), which are ozone and secondary organic aerosol precursors. Using the proton-transfer reaction time of flight mass spectrometer (PTR-ToF-MS) at an urban background site in Lucknow, the chemical characterisation of NMVOCs was performed in real-time from Dec-2020- May 2021. About ~173 NMVOCs from m/z 31.018 to 197.216 were measured during the study period, including aromatics, non-aromatics, oxygenates, and nitrogen-containing compounds. The campaign daily mean concentrations of the NMVOCs were  $125.5 \pm 37.5$  ppbv. The NMVOCs daily averaged concentrations average concentrations of NMVOCs are were about relatively ~30% high during winter months (December-February) than in summer (March-May). The oxygenated volatile organic compounds and aromatics were the dominant VOC families throughout the period, accounting for ~57-80% to the total NMVOCs concentrations. Acetaldehyde, acetone and acetic acid were the major NMVOCs species present 5-15 times higher than other species. An advanced multi-linear engine (ME-2) model was used to perform the NMVOCs source apportionment using positive matrix factorisation (PMF). It resolves the five main sources contributing to these organic compounds in the atmosphere. They include traffic (23.5%), two solid fuel combustion factors: SFC 1 (28.1%) and SFC 2 (13.2%), secondary volatile organic compounds (SVOC) (18.6%) and volatile chemical products (VCPs) (16.6%). Biomass burning contributes most to the NMVOCs and SOA formation, while interestingly, traffic sources most influence ozone formation. Aged and fresh emissions from Solid Fuel combustion (SFC 1 and 2) were the dominant contributor to total NMVOC and compounds related to these factors had a high secondary organic aerosols (SOA) formation potential. Interestingly, traffic factor is was the second highest contributor to total NMVOC and compounds related to this factor had high ozone formation potential. Significant differences in the composition of the two solid fuel combustion indicate the influence of local emissions and transport of regional pollution to the city. The high temperature during summer leads to more volatilisation of oxygenated VOCs, related to VCPs factor. The study is the first attempt to highlight the sources of NMVOCs and their contribution to secondary pollutants (SOA and O<sub>3</sub>) formations in Lucknow city during winter and summer seasons. The insights from the study would help various stakeholders in managing primary and secondary pollutants within the city.

Formatted: Font: 10 pt, Not Italic

Formatted: Font: Not Italic

Formatted: Font: (Default) Times New Roman, 10 pt

## 1. Introduction

Non-methane volatile organic compounds (NMVOCs) are carbon-containing gaseous compounds in the troposphere. NMVOCs can have significant effects (direct and indirect) on human health and the environment. These compounds have a half-life ranging from hours to months (Atkinson\*, 2000(Atkinson\*, 2000)(Atkinson\*, 2000)(Atkinson\*, 2000)(Atkinson\*, 2000)). Exposure (Inhalation or direct contact) to high levels of NMVOCs can produce multiple chronic and acute health effects on humans, including nose, eyes, throat, and liver irritation. NMVOCs like benzene, acrolein, and aromatic amines are carcinogens subject to long-term exposure (Balakrishnan et al., 2015; WHO, 2021).

The NMVOCs in the atmosphere act as precursors of ozone (O<sub>3</sub>) and secondary organic aerosols (SOA) (Hallquist et al., 2009; Monks et al., 2015(Hallquist et al., 2009; Monks et al., 2015)(Hallquist et al., 2009; Monks et al., 2015)(Hallquist et al., 2009; Monks et al., 2015). They are oxidised by

Formatted: Indent: First line: 0 cm

primary oxidant radicals such as hydroxyl radicals (OH), chlorine (Cl), and nitrate (NO<sub>3</sub>) in the presence of nitrogen oxides (NO<sub>x</sub>) and sunlight and can lead to the formation of ozone near the surface (Atkinson et al., 2004; Carter, 1994) and also secondary oxygenated volatile organic compounds (OVOCs) (de Gouw et al., 2005). These OVOCs undergo further oxidation, gaining polar functional groups or oligomerise and becoming less volatile. 55 When these compounds have sufficiently low vapour pressures, these products may condense to form a particle-phase secondary organic aerosol mass (Hallquist et al., 2009; Heald et al., 2008; Monks et al., 2009). The chemical composition of the parent compound, NO<sub>x</sub> concentrations and relative concentrations of OH and chloride radicals during the day and NO<sub>3</sub> during the night (Warneke et al., 2004) are factors that ultimately determine the fate of the formation of these aerosol products (Jang et al., 2002). At high NO<sub>x</sub> levels, VOCs degrade to form carbonyls, 60 hydroxy carbonyls, organic nitrates and peroxyacetyl nitrates (PAN). In contrast, low NO<sub>x</sub> conditions tend to produce fewer volatile compounds and organic peroxides after reaction with HO<sub>2</sub> radicals and favour SOA production from OVOCs. (Hallquist et al., 2009; Kroll et al., 2006; Ng et al., 2007; Xu et al., 2014).

65 The inherent complexity in the non-linear VOCs-NO<sub>x</sub>-O<sub>3</sub> relationship and change in ozone levels as a function of VOCs and NO<sub>x</sub> is understood by ozone isopleths. When VOCs are relatively high, and NO<sub>x</sub> is relatively low, ozone production is limited by NO<sub>x</sub>, which is considered a NO<sub>x</sub>-sensitive regime. Conversely, when VOCs are relatively low, and NO<sub>x</sub> is high, ozone production is determined by the concentration of VOCs and considered as VOC- sensitive regime (also known as a NO<sub>x</sub>-saturated regime) (Chameides et al., 1992). It is observed that the urban area of Delhi was frequently associated with VOC-sensitive chemical regimes (Sharma and Khare, 2017). The reduction of VOCs from anthropogenic emissions would reduce ozone levels more instead 70 of reducing NO<sub>x</sub> levels. (Sharma and Khare, 2017) also simulated that reducing NO<sub>x</sub> by 50% in Delhi would increase ground-level ozone production by about 10-50%. In contrast, it is recommended that strategies control abatement measures for NMVOCs, which would effectively reduce tropospheric ozone production by 60% more than abatement of ozone or particulate matter (PM<sub>2.5</sub>) alone.

75 The buildup of Surface ozone and SOA synergistically deteriorates the air quality and escalates harmful effects on humans and flora-fauna (Annenberg et al., 2018; Burnett et al., 2014; Pye et al., 2021). The increased PM<sub>2.5</sub> concentrations and other pollutants lead to economic and recreational loss, deterioration in the health of citizens, an increase in morbidity and premature mortality risks, and biodiversity loss. Extreme haze events are one of the major challenges for Indian cities, being among the most air-polluted cities in the world. Despite their importance, the spatial and temporal variability of the concentrations of NMVOCs, which are precursors to 80 secondary organic aerosols and ozone, remain unknown for most Indian cities. **The lack of identification of their sources and relative contribution remains a challenging task for policy driven measures.**

85 **Only a few studies have observed and reported the ambient NMVOCs levels in Indian cities. These studies are mainly conducted in large Indian cities such as Delhi** (Garg et al., 2019; Hoque et al., 2008; Srivastava et al., 2005; Tripathi et al., 2022), **Mumbai** (Srivastava et al., 2006), **Kolkata** (Chattopadhyay et al., 1997; Majumdar et al., 2011), **Ahmedabad** (Sahu et al., 2017, 2016; Tripathi and Sahu, 2020), **Udaipur** (Tripathi et al., 2021; Yadav et al., 2019), **and Mohali** (Sinha et al., 2014). **A previous study have presented the health risk assessments for ambient VOCs levels in Kolkata** (Chauhan et al., 2014; Majumdar (né Som) et al., 2008). **Most of these studies have examined only a few NMVOCs, mainly (BTEX), with less or no information related to their sources. Real-time characterization and source apportionment studies for NMVOCs in India are limited to national capital city of Delhi** (Jain et al., 2022; Stewart et al., 2021c; L. Wang et al., 2020), **and Mohali** (Pallavi et al., 2019) **across different seasons and sites. Traffic emissions and solid fuel combustion are observed to be major contributors in both cities. Significant contributions from secondary VOCs are found in Delhi while solvent based industries contributed to NMVOCs in Mohali. It is necessary to understand the different source profiles and source contributions to ambient NMVOCs in different cities. The atmospheric interactions with radicals, and meteorology** 95 **highly influence the concentrations of NMVOCs in the region.**

100 **Recent source apportionment studies based on real-time measurements of non-refractory fine particulate matter using HR-ToF-AMS identified various sources present at different sites in Delhi** (Lalchandani et al., 2021; Shukla et al., 2021; Tobler et al., 2020). **These studies emphasized that it is essential to understand the variance of sources between day-to-night and different seasons. The major contributors to fine suspended particulate matters in the National Capital Region are the burning of crop residues in neighboring states and open burning of waste, as well as the increased construction activities, industrial expansion, thermal power plants, number of vehicles (two-wheelers and cars), and residential fuel use that result from an ever-increasing population. In addition, recent studies based on real-time measurements of NMVOCs using PTR-ToF-MS in Delhi** (Jain et al.,

105 2022; L. Wang et al., 2020) and Mohali (Pallavi et al., 2019) emphasized the importance of source characterization of NMVOCs simultaneously. Very few source apportionment studies highlighted the sources of NMVOCs present in other Asian cities (Fukusaki et al., 2021a; Hui et al., 2018; Sarkar et al., 2017; Tan et al., 2021; Wang et al., 2021a). These studies highlighted that NMVOCs sources have substantial value in checking the secondary aerosols formation, and air quality.

110 The lack of identification of their sources and relative contribution of NMVOCs remains a challenging task for policy-driven measures. The development and evolution of strategies need an understanding of the seasonal and temporal variations and sources of NMVOCs. The reaction pathway is different for different NMVOCs and depends on the reaction rates of the species. Therefore, the ozone formation potential (OFP) of all NMVOCs is not the same. NMVOCs are categorised into distinct families based on their chemical structure and mass/charge (m/z) ratios. Some of these NMVOCs have lower OFPs than others and tend to form less ozone in the atmosphere. Understanding these OFPs in different chemical regimes would help identify families or species of NMVOCs of greater concern for surface ozone production control. [Source apportionment studies](#)

115  
120 Here, in this study, a real-time instrument, PTR-TOF-MS (Proton Transfer Reaction Time of Flight Mass Spectrometer)s is deployed for a period of 112 days (Dec-May) in Lucknow city, situated in the middle of the Indo-Gangetic plain, to understand the contribution of long-range transport and local VOC emissions. Lucknow, also known as the 'City of Nawabs', is an urban city situated in the center of the Indo-Gangetic Basin region. It is an urban city located on the banks of the Gomati River, and is the state capital of Uttar Pradesh, India. It is one of the fastest-growing cities and is now known for its manufacturing, commercial and retail hub. The exploding population due to increased migration from nearby towns and villages have widened the city boundaries. Currently, the city has two major Indian National Highways (NH-24 and NH-30) interjecting. The city has 125 petrol/diesel filling stations and seven designated industrial areas (*Brief Industrial Profile of District Lucknow, Uttar Pradesh*, 2018). The number of registered personal motor vehicles in the city as of 2017 is about ~2 million (Government of India, 2019), that had been increasing at an average rate of 9% every year since 2007. Besides this, 255 brick kilns operate within and around Lucknow city. Only ~4.7% of the area of the district is covered by forest area with ~ 2.8 million population (Census of India, 2011). The city has eight large-scale, public-sector undertakings, eleven medium-scale industries, and hundreds of micro, small and medium enterprises (MSMEs) (*Brief Industrial Profile of District Lucknow, Uttar Pradesh*, 2018). Increased industrial and construction activities, unregulated energy and fuel consumption, unchecked vehicular pollution and unsustainable urbanisation are major driving forces for poor air quality in Lucknow (*Uttar Pradesh Pollution Control Board*, 2019). The aerosol loadings in the city have been unprecedentedly high for the last two decades (Lawrence and Fatima, 2014; Markandeya et al., 2021; Sharma et al., 2006). The PM<sub>2.5</sub> concentrations were found to be highest in the industrial area during winter compared to residential and commercial spaces (Pandey et al., 2013, 2012). Lucknow is one of the fastest-growing cities and is now known for its manufacturing, commercial and retail hub. The exploding population due to increased migration from nearby towns and villages have widened the city boundaries. The number of registered personal motor vehicles in the city as of 2017 is about ~2 million (Government of India, 2019), that had been increasing at an average rate of 9% every year since 2007. Increased industrial and construction activities, unregulated energy and fuel consumption, unchecked vehicular pollution and unsustainable urbanisation are major driving forces for poor air quality in Lucknow (*Uttar Pradesh Pollution Control Board*, 2019). Nevertheless, minimal work has been carried out to investigate air pollution and its health impacts in the city, most of which are focused on particulate pollution. To our knowledge, there are no reported measurements of NMVOCs over the city.

130  
135  
140  
145 This study discusses the first-time ever measurements of NMVOCs using PTR-ToF-MS over the crucial site in the middle of the Indo-Gangetic basin (IGB). This study focuses on the relative source contribution of the different sources of the detected NMVOCs using positive matrix factorization (PMF) and their associations with organic aerosols. Recently developed and extensively used receptor Model, PMF for source apportionment studies can identify physically relevant environment factors robustly in comparison to other models (Paatero and Tapper, 1994, 1993). In present study, addition, the influence of meteorological parameters such as temperature, relative humidity, solar radiation to the diurnal and seasonal variation of NMVOCs is also studied. A specific goal of this study is to distinguish between primary emissions and secondary formations of NMVOCs. Moreover, the contribution of different sources of NMVOCs towards ozone and secondary organic aerosol formation is also estimated. The key highlight of the study is its comprehensive coverage of about 173

Formatted: Indent: First line: 0 cm

Formatted: Indent: First line: 0.63 cm

160 species of NMVOCs in the Lucknow city for two different seasons. As far as our knowledge, 173 different species of NMVOCs have not been reported elsewhere, in India. The insights from the results of the study would help the authorities in channelizing the strategies for the control of NMVOCs as well as formation of secondary pollutants (Ozone and SOA).

## 2. Methodology

### 2.1. Sampling site description

165 Lucknow, also known as the 'City of Nawabs', is situated in the centre of the Indo-Gangetic Basin. It is an urban city located on the banks of the Gomati River and is the state capital of Uttar Pradesh, India. Currently, the city has two major Indian National Highways (NH 24 and NH 30) interjecting. The city has 125 petrol/diesel filling stations and seven designated industrial areas (*Brief Industrial Profile of District Lucknow, Uttar Pradesh, 2018*). Besides this, 255 brick kilns operate within and around Lucknow city. Only ~4.7% of the area of the district is covered by forest area with ~2.8 million population (Census of India, 2011). The city has eight large-scale, public-sector undertakings, eleven medium-scale industries, and hundreds of micro, small and medium enterprises (MSMEs) (*Brief Industrial Profile of District Lucknow, Uttar Pradesh, 2018*). Most industrial and manufacturing plants are related to steel metal components and fabrication, automobile parts, chemical industries, food and agro-based and handicraft sectors (chikankari, zardozi, bone craft). The Industrial map of Lucknow and nearby districts with major/mini-industrial areas, large/medium scale industries, sewage treatment plants, solvent based industries, sugar mills, pharmaceutical industries, and power plants are shown in Figure 1.

170 175 The sampling site ( $26^{\circ} 51' 55.4''$  N,  $81^{\circ} 0' 17.5''$  E) is marked as a red triangle in Figure 1. It is located in Lucknow city at a height ~12 m above the ground in Uttar Pradesh Pollution Control Board (UPPCB) office building in Gomti Nagar. The sampling site is surrounded by residential buildings, office complexes, schools, big parks and commercial spaces. The most industrial and manufacturing plants within and around the city are related to steel metal components and fabrication, automobile parts, chemical industries, food and agro-based and handicraft sectors (chikankari, zardozi, bone craft). The Industrial map of Lucknow and nearby districts with major/mini-industrial areas, large/medium scale industries, sewage treatment plants, solvent based industries, sugar mills, pharmaceutical industries, and power plants are also shown in Figure 1. The measurements of NMVOCs were conducted using a proton-transfer-reaction time-of-flight mass-spectrometer (PTR-TOF-MS, Ionicon Analytik GmbH) from 18<sup>th</sup> December 2020 to 5<sup>th</sup> May 2021, covering winter and summer season. The study period is divided into two seasons according to the classification by IMD (Indian Meteorological Department) as winter (Dec-Feb) and summer (March-May). The instrument's inlet is connected to a Teflon PFA (perfluoroalkoxy) tube (1.5 m in length) for drawing air samples at the flow rate of 60 mL/min. The sampling was conducted from 18<sup>th</sup> December 2020 to 5<sup>th</sup> May 2021, covering three seasons: winter, spring, and summer. The gaps in the sampling period from 3-8<sup>th</sup> January and 21<sup>st</sup> March - 9<sup>th</sup> April are due to maintenance and calibration of the instrument. The average daily temperature is ~28 °C over the whole study period in the city. The mean daily temperature during winters (Dec-Feb) is around  $~25 \pm 2.5$  °C and during summers (March-May) is around  $32 \pm 3$  °C. The relative humidity ranges from 64±14% during winters and 42±11% during summers. The comparison of temperature and relative humidity changes during both seasons are shown as box plots in supplementary Figure 1. These values are based on the days when VOCs measurements exists. The pre-dominant wind direction is South, southeast during colder and southwest during warmer periods, as shown in supplementary Figure S2. The wind speed is relatively calm during winters than in summers. All the instruments were placed inside a temperature-controlled laboratory during the campaign. Detailed descriptions of the instruments can be found in subsequent sections.

### 2.2. Instrumentation and data analysis

#### PTR-ToF-MS measurements of NMVOCs

200 The PTR-TOF-MS is widely used for measuring NMVOCs with high mass resolution and sensitivity. A detailed description of the instrument can be found in other studies (Graus et al., 2010; Jordan et al., 2009; Tripathi et al., 2022; Tripathi and Sahu, 2020), while a brief description is given here. During The study, The the PTR-ToF-MS instrument's inlet is connected to a Teflon PFA (perfluoroalkoxy) tube (1.5 m in length) for drawing air samples at the flow rate of 60 mL/min. The PTR-TOF-MS is based on the chemical ionisation method, facilitated by proton-transfer reactions with hydronium ( $\text{H}_3\text{O}^+$ ) ions as the primary reactant ion, which causes much less fragmentation of organic molecules in the sampled air. The natural components of air (nitrogen, oxygen, hydrogen, carbon dioxide, Argon etc.) have a lower proton affinity than water molecules. They thus do not react with  $\text{H}_3\text{O}^+$ , while most VOCs have higher proton reactivity than water, facilitating non-dissociative proton transfer. These  $\text{H}_3\text{O}^+$  ions are generated with high efficiency (~99.5%) through a hollow cathode discharge source, and then these reactant ions enter the adjacent drift tube section. The sampled air is also injected into the drift tube section, where

210 proton transfer reactions between hydronium ions  $[H_3O^+]$  and neutral VOCs  $[R_iH_j]$  occur to form protonated product VOC ions  $[R_iH_{j+1}]$ , and water molecules  $[H_2O]$  as shown in equation 1. These  $[R_iH_{j+1}]$  then enter the orthogonal acceleration reflectron time-of-flight mass spectrometer via a specially designed transfer lens system (Jordan et al., 2009).



The parameters of the drift tube of the instrument were maintained at 2.2-2.4 mb, 60° C, 600 V, 130 Td for pressure, temperature, voltage and electric field (E/N; where E = electric field strength and N= gas number density) respectively and operated with a time resolution of 30 seconds. Typically, these or similar values have been observed as most suitable for ambient air measurements of NMVOCs (Blake et al., 2009, 2004). During The  
220 study, the PTR-ToF-MS instrument's inlet was connected to a Teflon PFA (perfluoroalkoxy) tube (1.5m in length) for drawing air samples at the flow rate of 60mL/min. The inner diameter of the tube was 0.075mm and the residence time of the inlet was less than 1 sec. The PTR-ToF-MS can identify hydrocarbons (HC) and oxygenated VOCs at sub-ppbv levels within a second (Graus et al., 2010; Müller et al., 2012). In this study, the PTR-ToF-MS measured 173 NMVOCs-ions (m/z 31.018 to 197.216) at the sampling site. The reaction rates (k) of the ions were applied from the literature (Cappellin et al., 2012). "A rate constant of  $2 \times 10^{-9} \text{ cm}^3 \text{ s}^{-1}$  was assumed for all ions which reaction rates (k) were not available in the literature (Smith and Spanel, 2005). The overall uncertainties were in the range of 8%–13% in the calculations of the mixing ratios of VOCs which were present in the standard mixture. The cause of uncertainties in the calculation VOC mixing ratios includes the uncertainties in the mass flow controllers (MFCs) of GCU and standard mixture ( $\pm 5\%–6\%$ ). The reaction rates (k) of the ion were applied from the literature (Cappellin et al., 2012). A rate constant of  $2 \times 10^{-9} \text{ cm}^3 \text{ s}^{-1}$  was assumed for all ions which reaction rates (k) were not available in the literature. (Hansel et al., 1999; Steinbacher et al., 2004) have reported up to 30% of uncertainty in the calculations of the mixing ratios of VOCs due to k reaction rate To compute the concentrations of VOCs, a typical value of  $2 \times 10^{-9} \text{ cm}^3 \text{ s}^{-1}$  of the proton transfer reaction rate coefficient (Smith and Spanel, 2005) has been employed. The calibration of the instrument was performed at the starting, middle and end of the campaign using a certified standard gas mixture (L5388, Ionicon Analytik GmbH Innsbruck, with a stated accuracy better than 8%) containing ~1.0 ppbv of VOCs. A detailed description of the calibration similar set-up and unidetails including zero measurement t is given in the previous studies (Jain et al., 2022; Tripathi et al., 2022), given in supplementary Figure . For method detection limits (MDL), we have calculated the MDL using  $3\sigma$  (standard deviation) of the zero air of 20 min time duration data points. The exact mass-identified chemical formula and family of species of the observed NMVOCs (173 in number) is given in supplementary Table S1. The mixing ratioconcentrations of these measured 173 NMVOCs-ions are averaged over the study period and compared in the box plots as shown in Supplementary Figure S2. The three most abundant NMVOC species are observed as acetaldehyde, acetone, and acetic acid.

### 245 2.3. Supporting measurements HR-ToF-AMS measurements of NR- $PM_{2.5}$

A high-resolution time-of-flight aerosol mass spectrometer (HR-ToF-AMS, Aerodyne Research Inc., USA) was also deployed for campaign measurements. HR-ToF-MS (Decarlo et al., 2006) measures size-resolved mass spectra of non-refractory  $PM_{2.5}$  (NR-  $PM_{2.5}$ ) with high time resolution (2 mins). A detailed description of the instrument can be found in other studies (Lalchandani et al., 2021; Shukla et al., 2021) and is explained briefly here. The ambient aerosols were sampled through the  $PM_{2.5}$  cyclone (BGI, Mesa Labs, Inc.) which gets transmitted through stainless steel tubing (~ 8 mm inner diameter and ~10 mm outer diameter) with a maintained flow. This setup is further connected to a Nafion dryer (MD-110-144P-4; Perma Pure, Halma, UK) to reduce moisture content and then it connects to the sampling inlet of the instrument. The ambient aerosols enter the aerodynamic lens through a sampling inlet (100  $\mu\text{m}$  diameter critical orifice) and focus on a narrow beam. This particle beam then enters a sizing chamber, where it is sorted based on its size. This size-resolved beam enters the vaporisation chamber, and the non-refractory part of the particles (Nr- $PM_{2.5}$ ) vaporises at 600° C and  $\sim 10^{-7}$  Torr. These gaseous molecules are then ionised and detected by a ToF-MS, depending on their m/z ratio. HR-ToF-AMS was operated in the high sensitivity V-mode for two cycles of 60s (total 2 minutes) regularly switching between MS and PTof mode for 30 seconds each. During the study period, the particles-free air was provided for 1-2 hours every week to check and correct the fragmentation table at m/z's 12, 16, 18, 29, 33, 40, 44. The IE (Ionization efficiency) calibrations were performed at the beginning, middle and end of the campaign study following using the mass-based method (Jayne et al., 1998)(Jayne et al., 2000) with a SMPS (scanning mobility particles sizer) unit (TSI Inc.). The raw data from HR-ToF-AMS was analysed for unit mass resolution (UMR) and high resolution (HR) using SQUIRREL (version 1.59) and PIKA (version 1.19) toolkit in Igor Pro software (version

220 Formatted: Not Highlight

225 Formatted: Font: (Default) Times New Roman, 10 pt, Font color: Auto, English (United States)

230 Formatted: Font: (Default) Times New Roman, 10 pt, Font color: Auto, English (United States)

235 Formatted: Font: (Default) Times New Roman, 10 pt, Font color: Auto, English (United States)

240 Formatted: English (United States)

245 Formatted: Not Highlight

250 Formatted: Font: Bold, Font color: Auto

265 6.37). The NR-PM<sub>2.5</sub> is chemically characterisedcharacterized intoby organics (Org), nitrates (NO<sub>3</sub>), sulphates (SO<sub>4</sub>), and chlorides (Cl). The organic aerosols mass spectra obtained from HR analysis and UMR analysis was combined from m/z 12 to 35000 (~545422 ions), to make the input matrix for PMF (positive matrix factorization) analysis. The PMF analysis was performed using a ME-2 engine over SoFi Pro (Source Finder, Datalystica Ltd., Switzerland) (Canonaco et al., 2013) in a graphical interface software Igor Pro version 6.37 (Wavemetrics, Inc., Portland).

270 Suggest separate section (2.3) HR ToF AMS measurements of aerosol composition providing more detail on HR ToF AMS measurements – aerosol inlet, calibrations, acquisition parameters, PMF

#### 275 2.4. Supporting measurements

280 An aethalometer (Magee Scientific, model AE-33) was also deployed at the campaign site to measure the real-time black carbon (BC) mass concentrations. It collects the aerosol particles samples on the quartz filter tape and quantifies the optical attenuation at seven different wavelengths (370, 470, 520, 590 660, 880 and 950 nm) with high temporal resolution (1 min). It is based on dual-spot technique for loading corrections (Drinovec et al., 2015). The change in optical attenuation measurements in the selected time interval at 880nm is converted to equivalent BC measurements (eBC) using the mass absorption cross section (MAC) of 7.77m<sup>2</sup> g<sup>-1</sup> (Drinovec et al., 2017, 2015). The Using the enhanced absorption of biomass burning aerosols in the near ultra-violet and bluewavelength range, the Aethalometer's multi-wavelength BC data may be apportioned into biomass burning and traffic combustion sources (Sandradewi et al., 2008; Zotter et al., 2017). The model employs an absorption ngströmexponent (AAE) value that corresponds to both vehicular and biomass combustion as the primary source of light-absorbing particles. In this study, AAE value of 0.9 for traffic, and 1.5 for biomass burning emissions based on previous studies (Vipul paper, anna Tobler). The More details about the instrument can be found in the previous studies (Lalchandani et al., 2021; Shukla et al., 2021, anna tobler). The sampling site (building) is a part of the national central ambient air quality monitoring stations (CAAQMS). The meteorological parameters (temperature, relative humidity, wind parameters) and concentrations of trace gases (NO<sub>2</sub>, SO<sub>2</sub>, Ozone) are downloaded from the CAAQMS dashboard (<https://app.cpcbccr.com/CCR/#/CAAQM-Dashboard-all/CAAQM-Landing>), managed by the central pollution control board (CPCB), government of India for Gomti Nagar station, Lucknow.

##### 285 2.4.2.5. Source apportionment

290 Numerous receptor models have been used to analyse the dynamic behaviour of ambient aerosol measurements and relate it to physical sources. One of the recently developed algorithms, positive matrix factorisation (PMF) (Paatero and Tapper, 1994), has been explored by numerous studies to apportion the measured bulk composition and temporal variation of aerosols (Talukdar et al., 2021; Zhang et al., 2011). The PMF algorithm is a non-negative, symmetrical factor analytic technique that produces unique factorisation by iterative reweighting of individual data values and unique solutions. It solves the common bilinear equation, given as (Eq. 2):

$$X (m \times n) = G (m \times p) F (p \times n) + E \quad (2)$$

300 where X represents the measured matrix, G and F are unknown matrices, and E is the error/ residual matrix. The m and n represent the time series and individual mass dimensions, and p is the number of factors. The calculated quantities G and F represent timeseries and profiles of the specific factor of the model solution, respectively. The ME-2 solver decreases the rotational ambiguity and fits the G and F entries to minimise the uncertainty in quantity 'Q'. This 'Q' is the sum of the squared residuals weighted by their respective uncertainties, as given in equation 3. From the equation, it can be inferred as a normalised chi-square metric, where e<sub>ij</sub> represents the residual matrix of E and σ<sub>ij</sub> represents measured data uncertainties.

$$Q = \sum_{i=1}^m \sum_{j=1}^n \left( \frac{e_{ij}}{\sigma_{ij}} \right)^2 \quad (3)$$

$$Q_{exp} = n \cdot m - p \cdot (m + n)$$

310 Another quantity, Q<sub>exp</sub>, degree of freedom, depends on the dimensions of the matrix and the number of factors. In an ideal case, the ratio of Q/Q<sub>exp</sub> is expected to be 1, with all the elements of the measured matrix and

Formatted: Font: (Default) Times New Roman, 10 pt

Formatted: List Paragraph, Outline numbered + Level: 2 + Numbering Style: 1, 2, 3, ... + Start at: 1 + Alignment: Left + Aligned at: 0.63 cm + Indent at: 1.9

Formatted: Font: 10 pt, Font color: Auto, English (United States)

Field Code Changed

Formatted: Not Superscript/ Subscript

Formatted: Not Superscript/ Subscript

Formatted: Font: 10 pt, Font color: Auto, English (United States)

uncertainties well-defined. However, it has been noticed in earlier studies that the absolute value of the ratio, Q/Q<sub>exp</sub>, is not always equal to 1 due to errors in measured data uncertainties, transient sources, and unknown model residuals. It is recommended to use relative change in this ratio and characteristics of the physical source while choosing the optimum factor solution (Paatero and Tapper, 1994, 1993). In this study, this algorithm is applied over the measured NMVOCs mass spectra using ME-2 (multi-linear engine) (Paatero, 1999) over SoFi Pro (Source Finder, Dataystica Ltd., Switzerland) (Canonaco et al., 2013) in a graphical interface software Igor Pro version 6.37 (Wavemetrics, Inc., Portland). Earlier studies have applied a similar PMF algorithm over mass spectra of 90 NMVOCs in Delhi (Jain et al., 2022; Wang et al., 2020) and 101 NMVOCs in Beijing (Wang et al., 2021). In this study, for the first time, we have included 170 NMVOCs measured by PTR-ToF-MS from m/z 42.034 to m/z 197.216. The input and residual error matrix for the PMF analysis were prepared using timeseries of mass spectra and calculated individual errors for each data point, as explained in the previous study (Jain et al., 2022). After incorporating the calibration factors, the uncertainties or residual error matrix is estimated by multiplying the peak area with the correction matrix. The total uncertainties vary in the range of 8-12% during calculations of the mixing ratio of NMVOCs. The three most abundant NMVOCs are not included in the PMF analysis due to their high signal-to-noise ratios and relatively higher (about 5-15 times) concentrations than other NMVOCs, as shown in supplementary Figure S2. The pretreatment of the input matrix also includes applying a minimum error threshold. The weak variables, having a signal-to-noise ratio <2 and bad variables, having a signal-to-noise ratio <0.2, are down-weighted by 2 and 10, respectively (Paatero and Hopke, 2003; Ulbrich et al., 2009).

Unlike the chemical mass balance (CMB) receptor model, the PMF algorithm itself calculates factor profiles. The most crucial decision for the interpretation of the findings of the PMF is selecting the optimum modelled number of factor solutions. This is achieved by applying several mathematical metrics, correlating with external measurements, and interpreting the physical sources. The ratio of Q/Q<sub>exp</sub> is first examined for every factor solution. The factor solution having an absolute value of Q/Q<sub>exp</sub> ratio near 1 indicates an accurate estimation of errors, and it should be selected but not observed for real observations. The Q/Q<sub>exp</sub> >> 1 and << 1 indicate under and overestimation of errors or variability in the factor solution, respectively. It is anticipated that Q will drop with each addition of the number of factors, as this introduces extra degrees of freedom to improve the fit of the data. Another important metric is the evaluation of scaled residuals as a function of timeseries and mass spectra. The scaled residuals  $\pm 3$  for each data point in the time series are considered, which is a evidence of a good quality PMF solution (Canonaco et al., 2021; Paatero and Hopke, 2003). The supplementary Figure S4 shows the scaled residuals over the timeseries and diurnal cycle for the 3-10 factor solution. In the present study, the Q/Q<sub>exp</sub> does not lie near 1, but the high % change in Q/Q<sub>exp</sub> is observed while examining 3-5 factor solutions, as shown in Figure 4. The total scaled residual of all species is calculated and plotted for different number of factors in Figure 4. The changes in the residuals and the drops in Q/Q<sub>exp</sub> indicate that the 5-factor solution is an optimum solution. This solution is further analysed regarding their mass spectral features, time series and correlation with external tracers (Org, NO<sub>3</sub>, SO<sub>4</sub>, Cl from Nr-PM<sub>2.5</sub>, organic resolved factors, gases (O<sub>3</sub>, NO, NO<sub>2</sub>, NO<sub>x</sub>, SO<sub>2</sub>), temp, RH, WD, WS, and BC concentrations).

The optimum factor solution from the PMF analysis was then further refined by self-constraining the secondary volatile organic compounds (SVOC) factor with random values varying from 0.1-1 with delta a= 0.1. Finally, a = 0.3 was chosen as the optimum solution after examining the temporal and diurnal variation of the factor. More details about the constraining of the solution is explained in Supplementary text ST1. Further, The uncertainty of the selected solution is quantitatively addressed by bootstrap analysis (Davison and Hinkley, 1997; Paatero et al., 2014), a module available in the SoFi Pro (Canonaco et al., 2021). Previous studies have also followed this methodology for uncertainty estimation of organic aerosols source apportionment (SA) results (Lalchandani et al., 2021; Tobler et al., 2020), elemental aerosols SA results, and VOCs SA results (Wang et al., 2021). The uncertainty or PMF<sub>error</sub> is observed as 1% or less for all factors Supplementary Figure S5. This infers that the 5-factor solution is a statistically robust solution with rather low uncertainty.

was chosen as explained in section 3.2 and correlated to external measurements (Org, NO<sub>3</sub>, SO<sub>4</sub>, Cl from Nr-PM<sub>2.5</sub>, organic resolved factors, gases (O<sub>3</sub>, NO, NO<sub>2</sub>, NO<sub>x</sub>, SO<sub>2</sub>), temp, RH, WD, WS, and BC concentrations).

#### 2.5.2.6. Ozone formation potential and SOA yield of NMVOCs

Ozone formation potential (OFP) is a reactivity-based estimation technique to assess the sensitivity of the VOCs for ozone formation (Carter, 2010, 1994). (e.g., (Tripathi et al., 2021)). The ground-level ozone is produced by photochemical reactions involving VOCs and NO<sub>x</sub>. The non-linear dependence of ozone formation on the

Formatted: Indent: First line: 0 cm

Field Code Changed

concentrations of  $\text{NO}_x$  and VOCs are described empirically by the ozone isopleths. Most Indian cities have high  $\text{NO}_x$  concentrations and lie in VOCs-sensitive regimes, i.e., oxidation of VOCs produces more radicals initiating ozone formation. Numerous VOCs are emitted into the atmosphere from various sources, followed by distinct reaction pathways and have different OFPs. The calculated reactivities of VOCs have been investigated in multiple computer modelling studies depending on the environmental conditions (Carter, 1994). This approach is based on calculating OFP using maximum incremental reactivity (MIR) values for individual VOC species, reported and updated by (Carter 2010), as given in the equation 4. MIR values are calculated as the change in ozone formed by adding a VOC to the base case in a scenario with adjusted  $\text{NO}_x$  concentrations. OFP of individual VOCs are estimated using Equation 4. Here, this equation is adopted (Carter, 2010, 1994) and modified for this study (Carter, 2010, 1994) to calculate the ozone formation potential for each of the factors, resolved from PMF analysis as given below (Eq. 54),

$$OFP(j) = [VOC_j] \times C_j \times MIR_j \quad (4)$$

$$OFP(i) = \sum_{j=0}^n [VOC_j] \times C_j \times RC_{ji} \times MIR_j$$


---

Where, OFP(j) and OFP(i) represents the ozone formation potential for an individual VOC (j) and a factor number (*i*) respectively, expressed in  $\mu\text{g}/\text{m}^3$ .  $[VOC_j]$  represents the mixing ratio (ppbv) of a given VOC ion (*j*),  $C_j$  is the number of carbon atoms present in each VOC ion (*j*),  $RC_{ji}$  is the relative contribution of VOC ion (*j*) to the factor (*i*).  $MIR_j$  is the maximum incremental reactivity of a VOC ion (*j*). The  $MIR_j$  are adopted from the (Carter, 2010, 2008, 1994). The above equation is used to compute the OFP for each factor and determine which source factor contributes the most to ozone generation, as explained later. The MIR values are available for a limited number (40 in number) of NMVOCs, given in supplementary Table S2. The NMVOCs without reported MIR values are not considered for OFP estimation.

The chemical pathways and reaction products involved in SOA formation from NMVOCs are poorly understood or even unknown. Estimation of SOA formation (SOA yield) has been largely constrained to indirect methods due to the complexity of the chemical matrix of organic aerosols and the lack of direct chemical analysis methods. Numerous studies have estimated SOA yield from different species involving computer modelling and chamber experiments (Zhang et al., 2017). The smog-chamber studies help estimate the value for SOA yield is more reliable as they mimic the actual scenarios. These parameters also helped in improving model parameterisation and SOA mitigation strategies. For the current study, the contribution of an individual NMVOCs species to SOA is estimated by multiplying the SOA yield by the concentration of the NMVOC species in the atmosphere (amount available for the reaction) as shown in Equation 6. The SOA yields  $Y_{SOA}$  (1) reported by Bruns et al 2016 were used for this analysis. The literature determines the SOA yield (Bruns et al., 2016). The compounds for which SOA yield values are not available from the literature directly, it is estimated that compounds having carbon atoms more than 6 (C > 6) will have the same SOA yield of 0.32 (Bruns et al., 2016). Based on their structure, the compounds (C > 6) are considered to contribute to SOA significantly (Bruns et al., 2016). The average value (0.32) of published SOA yield of 18 compounds (C > 6) is used. In this study, The individual SOA yield values considered is given in the supplementary Table S3. The contribution of the individual factor to SOA formation is also estimated using (Eq. 65 and 76) as given here.

$$C_{SOA}(j) = Y_{SOA(j)} \times VOC_j \quad (65)$$

$$C_{SOA}(i) = \sum_{j=0}^n VOC_j \times RC_{ji} \times Y_{SOA(j)} \quad (76)$$

Where,  $C_{SOA}(j)$  and  $C_{SOA}(i)$  represents the contribution to SOA formation for and individual VOC (j) and a factor number (*i*) respectively, expressed in  $\mu\text{g}/\text{m}^3$ .  $VOC_j$  represents the concentration ( $\mu\text{g}/\text{m}^3$ ) of a given VOC ion (*j*),  $RC_{ji}$  is the relative contribution of VOC ion (*j*) to the factor (*i*).  $Y_{SOA(j)}$  is the SOA yield of a VOC ion (*j*). This analysis represents the estimated OFP and SOA formation potential of the air mass composition at the sampling site, not the actual OFP and SOA formation potential from various sources. This means that if airmasses dominated by fresh emissions (e.g., traffic) will have a different OFP and SOA formation potential than aged airmasses (e.g., long range transport of BB plumes) or any other source.

The  $Y_{SOA}$  are adopted from (Bruns et al., 2016).

2.6. **CWT back trajectory** **Concentration weighted back trajectory analysis**

415 Concentrated-weighted backward trajectory (CWTBT) analysis determines the originating source and transport of air parcels at the receptor location within a specific period (Seiber et al., 1994, Draxler et al., 1998). The HYSPLIT model (v4.1 Hybrid Single Particle Lagrangian Integrated Trajectory) was used to perform the BT CWT analysis (Draxler et al., 2018; Stein et al., 2015). The 72-hour back trajectories with a 3-hour time interval at 100 m of arrival height above the ground were calculated using monthly GDAS (Global Data Assimilation System) files (ftp://arlftp.noaa.gov/pub/archives/gdas1) with a  $1^\circ \times 1^\circ$  resolution. The trajectories were calculated at 100 meters above ground level (AGL). To locate air masses based on their concentrations, the estimated backward trajectories (BTs) were weighted with VOCs factors time series and averaged over 3-h intervals using a concentration-weight trajectory (CWT) model. ZeFir (Petit et al., 2017), an IGOR-based interface, was used to construct the CWT graphs, as shown in supplementary Figure S3.

425 **3. Results and Discussions**

3.1. **NMVOCs concentration and temporal variation**

430 The average daily concentrations of measured NMVOCs during the study period is was  $125.5 \pm 37.5$  ppbv. Figure 2 shows the daily time series and monthly mean concentrations of NMVOCs, inorganics and organics fractions of Nr-PM<sub>2.5</sub>, O<sub>3</sub>, NO<sub>x</sub>, SO<sub>2</sub>, temperature, relative humidity, wind speed, and wind direction. Out of 173 detected ions of NMVOCs, the level of three major species (Acetaldehyde, acetone, and acetic acid) are were present 5-15 times higher than for other species, as shown in supplementary Figure S2. The monthly averaged concentrations of NMVOCs were observed relatively higher during winter months to decrease from December (193.7 ppbv) to January (110.2 ppbv) till March (101.2 ppbv) Feb (109.7 ppbv) than and increased sharply during the summer months, March (101.2 ppbv), April (137.8 ppbv) and May (150.8 ppbv). The highest averaged concentrations of NMVOCs (127±40 ppbv), as well as Nr-PM<sub>2.5</sub> (inorganics and organics) (102.8±51  $\mu\text{g}/\text{m}^3$ ) was higher, during the winter months, infer their common sources. The calm conditions and relatively lower planetary boundary layer during winters have slowed down the dispersion of the pollutants. In contrast, during the summer months, Nr-PM<sub>2.5</sub> (39.8±20  $\mu\text{g}/\text{m}^3$ ) decreased drastically, but NMVOC concentrations (122 ±32 ppbv) were similar to winters. This may be due to are relatively highest, implying additional sources of NMVOCs. High temperatures during warmer periods may lead to more photooxidation of primary VOCs (Sahu et al., 2017), production of biogenic VOCs (Baudic et al., 2016; Sahu et al., 2017) and evaporation of volatile household products (M. Qin et al., 2021). While aerosol particles managed to disperse in the atmosphere due to high planetary boundary layer and windy conditions. The difference of characteristics of the emission sources during both seasons may have also played an important role. During the winter period, the PM<sub>2.5</sub> exceeds most of the days than the NAAQS standard. PM<sub>2.5</sub> exceeds standards more frequently than ozone. Approximately, 80% of the days during the whole study period, PM<sub>2.5</sub> exceeds the NAAQS standards in the city, as shown in Figure 2.

A difference in temperature conditions during winters (colder) and summers (warmer) leads to more partitioning of the gas phase during summers relatively to winters.

450 The three abundant NMVOCs were not considered in the PMF analysis as explained in the section 2.5. The rest 170 nmvcos, considered for the PMF analysis varies from m/z 42. To. The average concentrations of these 170 NMVOCs was  $79.3 \pm 30.6$  ppbv. The averaged concentrations during winters were about  $86.7 \pm 35$  ppbv relatively more than during summers as  $68.3 \pm 17.2$  ppbv. summer to winters. These NMVOCs belong to different families based on their chemical composition. They are categorised as aromatics (Ar-CxHy), simple non-aromatics (N-CxHy), furans (Furans), phenols (Phenols), oxygenates: first (CHO<sub>1</sub>), second (CHO<sub>2</sub>), and third order (CHO<sub>3</sub>), nitrogen-containing compounds (CxHyNz and CxHyNzOn) and others. The others include high-order oxygenates (CHO<sub>4</sub>) and some hydrocarbons (CxHy). The degree of unsaturation (i.e. the number of rings and/or double bonds) of more than 4 distinguishes aromatics CxHy (ArCxHy) from the CxHy family. This allowed us to identify important VOCs markers, their families, and their role in their atmospheric chemistry. Overall, during the study period, highest contributing family belongs to oxygenates and aromatics. The CHO<sub>1</sub>, CHO<sub>2</sub> and CHO<sub>3</sub> families were 28.8% (~20.1 ppbv), 16.8% (11.7 ppbv), and 2% (1.4 ppbv) of total NMVOCs concentrations. The contribution from Ar-CxHy, and N-CxHy were about 21.5% (~15 ppbv), and 10.6% (~7.4 ppbv), respectively. Nitrogen containing compounds were relatively less present (~5.6% CxHyNz and 1.2% CxHyNzOn), 6.3% (~4.4 ppbv), and 3.7% (~2.6 ppbv) were contributed by Furans and Phenols at the site, rest were others (3.4%). ...The CPCB notified the annual National Ambient Air quality Standards (NAAQS) Only for benzene as 5 (~1.6 ppbv). While WHO recommended no safe level of exposure of benzene. The mean mixing

Formatted: Font: (Default) Times New Roman, Bold, English (United States)

Formatted: Font: (Default) Times New Roman, Bold, English (United States)

Formatted: Font: (Default) Times New Roman, Bold, English (United States), Not Expanded by / Condensed by

Formatted: Font: (Default) Times New Roman, Bold, English (United States)

Formatted: Font: (Default) Times New Roman, Bold, English (United States), Not Expanded by / Condensed by

Formatted: Font: (Default) Times New Roman, Bold, English (United States)

Formatted: Font: (Default) Times New Roman, Bold, English (United States), Not Expanded by / Condensed by

Formatted: Font: (Default) Times New Roman, Bold, English (United States)

Formatted: Normal, No bullets or numbering

Formatted: Font: 10 pt, Not Italic, Font color: Auto, English (United States), Do not check spelling or grammar

Formatted: Font: 10 pt, Not Italic, Font color: Auto, English (United States), Do not check spelling or grammar

Formatted: Font: 10 pt, Not Italic, Font color: Auto, English (United States), Do not check spelling or grammar

Formatted: Font: 10 pt, Not Italic, Font color: Auto, English (United States), Do not check spelling or grammar

Formatted: Not Highlight

ratio of benzne during the study period found to be ... 2.9  $\pm$  1.9 ppbv which is 25–10 times higher than the standard guidelines. Prolonged exposure or high short-term exposure to benzene adversely affect the health of citizens of the city due to its haematotoxic, genotoxic and carcinogenic properties.

470

All three abundant NMVOCs present at m/z 45.034 ( $C_2H_5O$ , acetaldehyde), 59.049 ( $C_3H_7O$ , acetone), and 61.028 ( $C_2H_5O_2$ , acetic acid) are oxygenated VOCs (OVOCs). The sources of these OVOCs could be direct emissions from biogenic and anthropogenic activities and from the secondary/ photochemical processes also. Diurnal variations of secondary formation, anthropogenic emission level, meteorological conditionsweather, and PBL heights influence can be explained by OVOCs/benzene ratios (Sahu et al., 2017, 2016; Tripathi et al., 2022) to some extent. The diurnal patterns of acetaldehyde/benzene, acetone/benzene, and acetic acid/benzene ratios are plotted to check the influence of biogenic and secondary sources (see Figure 3 (a-c)). All the OVOCs/Benzene ratios are observed to increase during the daytime (10–18 h), similar to temperature variation. This infers the influence of photochemical formation and/or biogenic emissions of these compounds. The elevated OVOCs concentrations during the night confirm the influence of anthropogenic emissions.

475 Acetone and acetaldehyde are formed during photooxidation and ozonolysis of various terpenes and aromatics compounds emitted from multiple biogenic and anthropogenic sources (Lee et al., 2006a, 2006b; S. Wang et al., 2020). Acetone plays a major role in Ozone production. It can be transported to remote areas due to its long lifetime in the troposphere (~15 days) (Seco et al., 2007). The average concentrations of acetone during winters, late winters and summer were observed as  $13.6 \pm 4.5$  ppbv,  $15.3 \pm 5.4$  ppbv and  $34.9 \pm 10.3$  ppbv, respectively. The observed concentrations of acetone in Lucknow are on the higher side of the range of measured concentrations in other Indian cities. The reported average concentrations of acetone in the present study are comparable to Delhi (whole year) is  $\sim 16.7$  ppbv (13–15 ppbv during winters) (Jain et al., 2022) but higher than Ahmedabad at  $5.35 \pm 1$  ppbv during late winters (Sahu et al., 2016), and Mohali as  $5.9 \pm 3.7$  ppbv during summers (Sinha et al., 2014). This shows the presence of more OVOCs in cities within the IGB region than in other cities of India.

480 As shown in Figures 3 (a) and 3 (b), the diurnal variation of acetaldehyde and acetone, respectively, starts increasing from 9 h in the morning to 16 h in the evening. The acetaldehyde and acetone had their morning maxima at around 10:00 LT and 11:00 LT, respectively, and later during the morning rush hours of vehicular emissions (8–10 h). This trend is similar to a previous study in Ahmedabad (Sahu and Saxena, 2015). It indicates the secondary formation of acetone and acetaldehyde from terpenes and aromatics emitted from vehicles. The OH reaction rate constant of the hydroxyl radical with acetaldehyde ( $15 \times 10^{-12} \text{ cm}^3 \text{ molecule}^{-1} \text{ s}^{-1}$ ) is significantly higher than the reaction rate constant of the hydroxyl radical with acetone ( $0.17 \times 10^{-12} \text{ cm}^3 \text{ molecule}^{-1} \text{ s}^{-1}$ ), indicating faster degradation of acetaldehyde than acetone (Atkinson and Arey, 2003).

485 Figure 3 (c) shows the diurnal variation of acetic acid and acetic acid/ benzene ratio. Acetic acid is one of the most abundant VOC species in the atmosphere globally, having a half-life of more than one day. It contributes to atmospheric acidity (Chebbi and Charlie, 1996) and is responsible for 30% acidity of the wet deposition in polluted urban areas ( Seco et al., 2007, Pena et al., 2002). This compound also has toxic effects on 490 human health. Residential wood combustion is one of the critical sources of acetic acid (Bruns et al., 2017). High levels of acetic acid have also been reported from aged open biomass (hay and straw) burning plumes (Brilli et al., 2014), a variety of biomass fuel (Stockwell et al., 2015), and natural gas (Gilman et al., 2013). The average concentration of acetic acid during the whole study period is about  $10.3 \pm 4.1$  ppbv, highest during winters at  $15.2 \pm 3.5$  ppbv and lower during summers at  $6.9 \pm 2.1$  ppbv. The observed increased concentrations of acetic acid in 495 the winter and lower concentration in the summer may demonstrate its production influenced by open biomass burning crops in nearby fields and residential wood combustion for heating and cooking purposes in Lucknow. The diurnal pattern of acetic acid concentrations shows high concentrations during the night, which infers its 500 accumulation.

### 3.2. Characteristics of selected PMF factorsPMF results

505 This section includes a discussion of the selection of the source apportionment solution and its interpretation. The NMVOCs factors are identified based on their mass spectra, diurnal and temporal variation, and correlation with external tracers. For the first time, we have included mass spectra of 170 NMVOCs ions from m/z 42. 034 to m/z

510 Formatted: Indent: First line: 0 cm

197.216 in the PMF analysis. The three abundant NMVOCs (compounds below m/z 42), detected by PTR-ToF-  
520 MS, acetaldehyde, acetone, and acetic acid are not included from PMF analysis. Including these NMVOCs in the PMF analysis, resulted in biased solutions where only these ions are well-explained. Additionally, few small alkanes and alkenes (C1-C4) compounds, which are not detected by PTR-ToF-MS are excluded from PMF analysis. However, previous studies have found that these ions are minor contributors to SOA formation. Included compounds (above m/z 42) are major contributors to SOA formation and dominant markers of various sources.  
525 These ions belong to different families based on their chemical composition. They are categorised as aromatics (Ar-CxHy), simple non aromatics (N-CxHy), furans (Furans), phenols (Phenols), oxygenates: first (CHO<sub>2</sub>), second (CHO<sub>3</sub>), and third order (CHO<sub>4</sub>), nitrogen-containing compounds (CxHyNz and CxHyNzOn) and others. The others include high order oxygenates (CHO<sub>5</sub>) and some hydrocarbons (CxHy). The degree of unsaturation (i.e. the number of rings and/or double bonds) of more than 4 distinguishes aromatic CxHy (ArPh-CxHy) from the CxHy family. This allowed us to identify important VOCs markers, their families and their role in their atmospheric chemistry. As explained in section 2.4, the optimum solution after the PMF analysis chosen is 5-factor solution. This selected 5-factor PMF solution exhibits distinct mass spectral characteristics related to different sources and atmospheric processes. Figure 5 shows the intricate plots of the profile and diurnal variation of the 5-factor solution. The five factors are Traffic, SFC 1 (solid fuel combustion), SVOC (secondary volatile organic compounds), SFC 2, and VCPs (volatile chemical products) after thoroughly investigating markers, chemical species and their families, diurnal variation, and relation to meteorological parameters and external measurements.  
530  
535

The timeseries of the five factors resolved from NMVOCs mass spectra are co-related with external measurements such as oxygenated organic aerosols (OOA), Black carbon (BC) concentrations, CAAQMS data (WD, WS, RH, Temp, NO, NO<sub>2</sub>, NOX, SO<sub>2</sub>, Ozone) as given in Figure 8.

Formatted: Indent: First line: 0.63 cm

### 3.2.1. Optimum solution selection

Unlike the chemical mass balance (CMB) receptor model, the PMF algorithm itself calculates factor profiles. The most crucial decision for the interpretation of the findings of the PMF is selecting the optimum modelled number of factor solutions. This is achieved by applying several mathematical metrics, correlating with external measurements, and interpreting the physical sources. The ratio of  $Q/Q_{exp}$  is first examined for every factor solution. The factor solution having an absolute value of  $Q/Q_{exp}$  ratio near 1 indicates an accurate estimation of errors, and it should be selected but not observed for real observations. The  $Q/Q_{exp} \gg 1$  and  $\ll 1$  indicate under- and overestimation of errors or variability in the factor solution, respectively. It is anticipated that  $Q$  will drop with each addition of the number of factors, as this introduces extra degrees of freedom to improve the fit of the data. Another important metric is the evaluation of scaled residuals over timeseries and mass spectra. The scaled residuals  $\pm 3$  for each data point in the time series are considered. The supplementary Figure S4 shows the scaled residuals over the timeseries for the 3-7 factor solution. In the present study, the  $Q/Q_{exp}$  does not lie near 1, but the high % change in  $Q/Q_{exp}$  is observed while examining 3-5 factor solutions, as shown in Figure 4. The total scaled residual of all species are calculated and plotted for different number of factors in Figure 4. The changes in the residuals and the drops in  $Q/Q_{exp}$  indicate that the 5 factor solution is an optimum solution. Below, this solution is further analysed regarding their mass spectral features, time series and correlation with external tracers.  
540  
545  
550  
555

For further assurance of our chosen solution, the whole dataset was divided into three periods; winter (December), late winter (Jan-march) and summer (April-may). The unconstrained PMF was performed on each period for 2-12 factors and analysed further. The SVOC factor from the unconstrained solution during the late winter period was used to constrain the same factor for the whole period. The constrained profile of SVOC was used for self constraining with random values varying from 0.1-1 with delta  $\alpha = 0.1$ . Finally,  $\alpha = 0.3$  was chosen as the optimum solution after examining the temporal and diurnal variation of the factor. The SVOC factor's constraining helped improve the diurnal variation, which enhanced the confidence in the selected solution.  
560

The uncertainty of the selected solution is quantitatively addressed by bootstrap analysis (Davison and Hinkley, 1997; Paatero et al., 2014), a module available in the SoFi Pro (Canonaco et al., 2021). Previous studies have also followed this methodology for uncertainty estimation of organic aerosols source apportionment (SA) results (Lalchandani et al., 2021; Tobler et al., 2020), elemental aerosols SA results, and VOCs SA results (Wang et al., 2021). This assessment involves randomly resampling the original input data and generating new input data matrices for each run. The variation within the identified factors across all bootstrapped runs allows for estimating the statistical uncertainty if enough resamples have been conducted. For the study, the number of resamples is kept at n=500 iterations to check the robustness of the 5-factor solution. Each factor's base case time series was fed into  
565  
570

Formatted: Indent: First line: 0 cm

Field Code Changed

the model to check the variance with each bootstrapped run. Then, based on pre-defined criteria for individual factors, it is observed that 476 out of 500 runs were accepted with a correlation coefficient above 0.9 and a p-value lower than 0.05. The reported individual mass estimation error for PMF analysis  $PMF_{error}$ , for individual factors ( $i$ ) is calculated by the linear fit method using equation given below (Eq. 7).

575 
$$PMF_{error, i} = 100 \times \left( \frac{\text{spread}}{\text{mean}} \right) \quad (7)$$

Where the spread may refer to the standard deviation and the mean is the averaged concentration of the factor. A linear fit's slope indicates relative inaccuracy when comparing the spread to the mean value. The uncertainty or  $PMF_{error}$  is observed as 1% or less for all factors (Supplementary Figure S5). This infers that the 5-factor solution is a statistically robust solution with rather low uncertainty.

Formatted: Indent: First line: 0 cm

580 **3.2.2.3.2.1. Profile and diurnal variation Factor 1: Traffic**

The selected 5-factor PMF solution exhibits distinct mass spectral characteristics related to different sources and atmospheric processes. Figure 5 shows the intricate plots of the profile and diurnal variation of the 5-factor solution. The five factors are Traffic, SFC 1 (Solid Fuel Combustion), SVOC (Secondary volatile organic compounds), SFC 2, and Industrial after thoroughly investigating markers, chemical species and their families, diurnal variation, and relation to meteorological parameters and external measurements. The first factor is identified as traffic. It is characterized by the presence of aromatics, such as benzene (m/z 79.053,  $C_6H_6H^+$ ), toluene (m/z 93.07,  $C_7H_8H^+$ ), xylene (107.09,  $C_8H_{10}H^+$ ), C9-aromatics (121.1,  $C_9H_{10}H^+$ ), and C10-aromatics (135.12,  $C_{10}H_{11}H^+$ ). 56% of the total aromatics are explained by this factor, as shown in Figure 6. The explained variation of individual NMVOCs, such as  $C_6H_6H^+$ ,  $C_7H_8H^+$ , and  $C_8H_{10}H^+$  by the traffic factor is around 0.56, 0.77, and 0.76, respectively, as shown in Figure 7 (a). The NMVOC's traffic factor shows a temporal correlation (Pearson  $r^2 \sim 0.7443$ ) with nitrogen oxides ( $NO_x$ ), which is also an indicator of vehicular emissions (Figure 8). This infers the  $NO_x$  emissions along with NMVOCs from the vehicular fleet. Also, this factor has a good correlation (Pearson  $r^2 \sim 0.65$ ) with the AMS HOA (PMF-resolved factor from HR-ToF-AMS), as shown in Figure 9 (a). This AMS HOA factor is characterized by aliphatic hydrocarbons, typically associated with traffic exhaust emissions (Lalchandani et al., 2021). It infers that vehicular exhaust is one of the common sources influencing the release of NMVOCs,  $NO_x$  and primary OA. These NMVOCs and primary OA also exhibit similar diurnal variation, having sharp peaks during morning and evening hours, as shown in supplementary Figure S7. These diurnal pattern indicates the vehicular commute pattern in the city, high density of vehicles on the roads variation shows peaks during rush hours in the morning and evening. The diurnal pattern is compared between two seasons, winters and summers, also shows similar pattern in supplementary Figure S3. The traffic factor in previous studies observed similar markers and diurnal pattern in Delhi (Jain et al., 2022; Wang et al., 2020) and Beijing (Wang et al., 2021b), indicating the similar commute pattern in most of the urban cities. Other source-specific studies also identified similar markers for vehicular emissions (Cao et al., 2016; Caplain et al., 2006). The dominant markers in its mass spectra belong to the family of aromatics (~56%), as shown in Figure 6. The back trajectory analysis of the factor, (The CWT graph), as shown given in Supplementary Figure S3, shows the probable sources of traffic present near the sampling site.

590 **3.2.2. Factor 2: Solid Fuel Combustion (SFC 1)**

Formatted: Font: (Default) Times New Roman, 10 pt

600 Another factor which is resolved is Solid Fuel Combustion (SFC 1), have has the highest contribution from furans and substituted furans (~36%) and nitrogen-containing compounds (34%), as shown in Figure 5. Furans and nitrogen-containing compounds are mostly emitted from combustion processes (Coggon et al., 2019), cooking fires, burning of peat, crop residue and biomass fuel such as wood, grasses etc. (Stockwell et al., 2015). Studies have also shown that furans and nitrogen-containing compounds have a high potential to form secondary organic aerosols and particles. The prominent signals of acrylonitrile (m/z 54.034,  $C_3H_4N$ ), furan (m/z 69.033,  $C_4H_6O$ ), pyridine (80.054,  $C_5H_6N$ ), furfurals 81.036,  $C_5H_5O$ , furaldehyde (m/z 97.027,  $C_5H_5O_2$ ), dimethyl furan (97.064,  $C_6H_9O$ ), and  $C_3H_3N_2O_3$  (115.012) also contribute to the factor's mass spectra as shown in Figure 7 (a). This factor profile is characterized by the strong peak of acetonitrile (m/z 42.034,  $C_2H_4N$ ) with an explained variation of about ~0.49, as shown in Figure 7 (b). Acetonitrile is considered a unique marker of biomass burning (Holzinger et al., 1999). Furans and nitrogen-containing compounds are mostly emitted from combustion processes (Coggon et al., 2019), cooking fires, burning of peat, crop residue and biomass fuel such as wood, grasses etc. (Stockwell et al., 2015). Studies have also shown that furans and nitrogen-containing compounds have a high potential to form secondary organic aerosols and particles. Other markers, The nitrophenol (m/z 140.033,  $C_6H_6NO_3$ ) and methoxy nitrophenol (m/z 154.054,  $C_7H_8NO_3$ ) is-are explained by SFC 1 factor profile of ~0.53

Formatted: List Paragraph, Outline numbered + Level: 3 + Numbering Style: 1, 2, 3, ... + Start at: 1 + Alignment: Left + Aligned at: 0.63 cm + Indent at: 1.9

610 Formatted: Not Highlight

615 Formatted: Not Highlight

620 Formatted: Not Highlight

Formatted: Not Highlight

Formatted: Not Highlight

and 0.52, respectively. It is reported that phenols in a biomass smoke plume react with NO<sub>x</sub> to form nitrophenol, considered a unique marker for aged biomass burning smoke (Harrison et al., 2005; Mohr et al., 2013).  
625 Nitrophenols and other nitrogen-containing aerosols act as cloud condensation nuclei (Kerminen et al., 2005; Laaksonen et al., 2005; Sotiroglou et al., 2006), and contribute to the formation of SOA and light-absorbing brown carbon aerosols (Laskin et al., 2009; Mohr et al., 2013). SFC 1 factor correlates with organics fraction of Nr-PM<sub>2.5</sub> (Org\_Hr), NO<sub>3</sub>\_Hr (inorganics NO<sub>3</sub> of Nr-PM<sub>2.5</sub>) and RH well with Pearson r<sup>2</sup> ~ 0.46, 0.53, and 0.47, respectively. The SFC factors resolved from organic mass spectra contained significant signals from unsaturated hydrocarbons, polyaromatic hydrocarbons, and oxygenated fragments (Lalchandani et al., 2021; Shukla et al., 2021). The AMS SFC/OA factor relates to the primary emissions from the combustion process of wood and paper, and biomass is influenced by a higher O/C (~0.878) ratio than the AMS SFC/BB O/C ratio (~0.268). The resolved factor from VOCs mass spectra related to biomass burning (SFC 1) shows a strong temporal correlation (Pearson r<sup>2</sup> ~ 0.85) with AMS SFC/OA. Thus, we interpret SFC 1 as more related to conventional biomass burning at the site. The diurnal pattern of the SFC 1 from NMVOCs (Figure 5), shows peaks during cooking times, morning (7:00-8:00) and evening (19:00-21:00). The correlation of SFC 1 with organics Nr-PM<sub>2.5</sub> This argues that The domestic usage of biomass for cooking and other purposes is one of the leading factors for primary emissions of gas-phase (SFC 1) and particle-phase oxygenates (OOA). This factor may belong to the aged biomass burning plume, transported from sources located on the outskirts of the city and nearby districts. The city is surrounded by various agricultural fields, which generally involve open biomass burning activities. The back trajectory analysis of the factor also shows the probable sources in nearby areas, mainly coming from the west direction of the sampling site (supplementary Figure S3). This argues that this factor is also influenced by may belong to the aged biomass-burning plume, transported from sources located on the outskirts of the city and nearby districts.

#### 645 3.2.3. Factor 3: Solid Fuel Combustion (SFC 2)

The third factor, Solid Fuel Combustion (SFC 2), was identified in the 5-factor solution. The unique characteristic of this factor is its presence only in December only. Lower ambient temperature and high relative humidity during this month are responsible for the different chemical pathways for the fate of compounds. The factor's mass spectra is characterized with peak signals of methyl furan (m/z 83.049, C<sub>5</sub>H<sub>7</sub>O), phenol (m/z 95.049, C<sub>6</sub>H<sub>5</sub>O), cresol (m/z 109.06, C<sub>7</sub>H<sub>9</sub>O), catechol (m/z 111.043, C<sub>6</sub>H<sub>6</sub>O<sub>2</sub>), phenyl butanediol (m/z 163.115, C<sub>10</sub>H<sub>11</sub>O<sub>2</sub>), hexene (m/z 85.093, C<sub>6</sub>H<sub>13</sub>), as shown in Figure 5 (a). The SFC 1 and SFC 2 factor profile is compared with each other in Figure 7 (a). It explains the similar NMVOCs are present in the factors, but the intensity of the signal is different. This is due to the difference in the emission sources and chemical pathways of formation. Lower ambient temperature and high relative humidity during this month are responsible for the different chemical pathways for the fate of compounds. For example, High molecular weighted and more substituted phenolic compounds such as guaiacol (m/z 125.059, C<sub>7</sub>H<sub>9</sub>O<sub>2</sub>) and cresol are released at the early stages of the smouldering stage of the fire (lower temperature), and low molecular weighted phenols are released during later stages (high temperature) (Stewart et al., 2021a). The higher explained variation from cresol (~0.8) and guaiacol (0.21) to the factor's profile indicate their new emissions from residential heating activities and the burning of sawdust (Stewart et al., 2021a), as shown in Figure 7 (b). Other compounds like phenols (0.27) and hexene (~0.62) are explained by this SFC 2 factor's profile. These two compounds are being reported in the emissions from local biomass burning of wood in an Indian city (Delhi) (Stewart et al., 2021).

665 The factor profile explains 53% of phenols, 23% of second-order oxygenates, 30% of furans and 21% of nitrogen-containing compounds, are also present in the factor profile. Commonly used domestic fuels other than liquid petroleum gas (LPG) in the Indian sub-continent are cow dung, fuelwood, and peat, in different proportions depending upon their composition and availability. A previous study (Stewart et al., 2021b) observed phenols are released from the combustion of fuelwood (22-80%), followed by crop residue (32-57%), cow dung cake (32-36%), and municipal solid waste (24-37%). The combustion process at a higher temperature leads to the depolymerisation of lignin content in the biomass, which allows the aromatisation process to give off phenols, substituted phenolic compounds, and non-substituted aromatics (Sekimoto et al., 2018; Simoneit et al., 1993). The lower ambient temperature during December is also responsible for increased burning activities for cooking and heating purposes. The diurnal variation of SFC 2 shows its prominence during evening hours and accumulation during late evening (21:00) till mid night. The correlation coefficient between SFC 2 and black carbon concentrations is ~0.4. The factor SFC 2, derived from the VOC mass spectra, is less related (Pearson r<sup>2</sup> ~0.38)

670 Formatted: Font: (Default) Times New Roman, 10 pt

675 Formatted: List Paragraph, Outline numbered + Level: 3 + Numbering Style: 1, 2, 3, ... + Start at: 1 + Alignment: Left + Aligned at: 0.63 cm + Indent at: 1.9

680 Formatted: Indent: First line: 0 cm

to the AMS MO-OOA as shown in Figure 9 (c) and supplementary Figure S7. AMS MO-OOA is characterised by higher m/z 44 ( $\text{CO}_2$ ) and m/z 43 ( $\text{C}_2\text{H}_3\text{O}$ ) fractions than the primary OA sources. This factor is comparatively more oxidised, having an O/C ratio of ~0.89 than AMS LO-OOA (O/C ratio ~0.62). ~~Welt~~ may be interpreted that SFC 2 is influenced by fresh oxidation of primary biomass burning emissions. Moreover, the CWT plots as shown in supplementary Figure S3, no evidence of its long-range transport is present.

The factor's mass spectra is characterized with peak signals of methyl furan (m/z 83.049,  $\text{C}_8\text{H}_8\text{O}$ ), phenol (m/z 95.049,  $\text{C}_6\text{H}_5\text{O}$ ), cresol (m/z 109.06,  $\text{C}_8\text{H}_9\text{O}$ ), catechol (m/z 111.043,  $\text{C}_6\text{H}_6\text{O}_2$ ), phenyl butanedione (m/z 163.115,  $\text{C}_{10}\text{H}_{12}\text{O}_2$ ), hexene (m/z 85.093,  $\text{C}_6\text{H}_{12}$ ), as shown in Figure 5 (a). The SFC 1 and SFC 2 factor profile is compared with each other in Figure 7 (a). It explains the similar NMVOCs are present in the factors, but the intensity of the signal is different. This is due to the difference in the emission sources and chemical pathways of formation. For example, High molecular weighted and more substituted phenolic compounds such as guaiacol (m/z 125.059,  $\text{C}_8\text{H}_9\text{O}_2$ ) and cresol are released at the early stages of the smouldering stage of the fire (lower temperature), and low molecular weighted phenols are released during later stages (high temperature) (Stewart et al., 2021a). The higher explained variation from cresol (~0.8) and guaiacol (0.21) to the factor's profile indicate their new emissions from residential heating activities and the burning of sawdust (Stewart et al., 2021a), as shown in Figure 7 (b). Other compounds like phenols (0.27) and hexene (~0.62) are explained by this SFC 2 factor's profile. These two compounds are being reported in the emissions from local biomass burning of wood in an Indian city (Delhi) (Stewart et al., 2021)

#### [.Factor 4: Secondary volatile organic compounds \(SVOC\)](#)

The fourth factor, secondary volatile organic compounds (SVOC), has the highest contribution from second-order oxygenates (40 %) and third-order oxygenates (40%), as shown in Figure 6. The relative composition of the profile of the factor reveals significant signals of acetic acid (m/z 77.019,  $\text{C}_2\text{H}_5\text{O}_2$ ), propylene glycol (m/z 77.048,  $\text{C}_3\text{H}_6\text{O}_2$ ), methylglyoxal (m/z 73.028,  $\text{C}_3\text{H}_5\text{O}_2$ ), methyl methacrylate (93.033  $\text{C}_6\text{H}_8\text{O}$ ), and  $\text{C}_5\text{H}_8\text{O}_2$  (m/z 101.059). Lower contributions from first-order oxygenate than the second, and third-order oxygenates indicate that these OVOCs are products of various photochemical and oxidation processes in the atmosphere instead of their direct emissions. The diurnal mean concentration of the SVOC factor in Figure 5 (b) shows distinct day-to-night variation, following the pattern of solar radiation. The mean concentration increases during the morning (8:00), peaks during the afternoon hours (12:00-15:00), and decreases towards the evening (20:00). The nighttime concentration of the factor is lowest due to the absence of photochemical activity at night. Small organic acids like formic acid (m/z 47.012,  $\text{CH}_3\text{O}_2$ ) could potentially come from the photooxidation of furans and aromatics (Stewart et al., 2021a; Wang et al., 2020), which contribute 42.2% to the SVOC factor's profile (Figure 6). Other compounds like methoxyphenols are released by biomass burning, which is further photo-oxidised, resulting in the formation of SOA (Li et al., 2014; Yee et al., 2013). Figure 7 (b) shows the explained variation of these compounds, such as vanillin (methoxyphenol) and syringol (2,6-dimethoxyphenol) to the SVOC factor is ~0.57 and 0.41, respectively, relatively high. This also confirms the association of products and intermediate products of photochemical reactions with the SVOC factor. The temporal variation of this factor has no significant correlation with any of the AMS factor or external tracers.

#### [3.2.4. Volatile chemical products \(VCPs\)](#)

The Volatile Chemical products (VCPs) factor is identified with prominent signals of formaldehyde (m/z 31.018,  $\text{CH}_2\text{O}$ ), ethanol (m/z 47.049,  $\text{C}_2\text{H}_5\text{O}$ ), and naphthalene (m/z 129.05,  $\text{C}_{10}\text{H}_8$ ). 62.4% and 76.6% of the formaldehyde and ethanol contribute to the VCPs factor. Volatile chemical products show good temporal correlation with a solvent-based NMVOCs species. Acetone, with Pearson  $r^2 \sim 0.6$ . Formaldehyde and ethanol are used as solvents in the paint, solvent-based, textile, plastics, and automobile industries. Formaldehyde is also commonly used as an industrial disinfectant, fungicide, and germicide. 62.4% and 76.6% of the formaldehyde and ethanol contribute to the industrial factor. Many such kind of industries (solvent-based and textile) are present in the close vicinity of the sampling site, which is possibly the reason for the high concentration of formaldehyde and ethanol. Shorter-life spans of formaldehyde (~1 hour) and ethanol (~3-4 hours) in the atmosphere confirms their its emissions from local source instead of transport from regional sources. The relative contribution of naphthalene is about 28.3%, respectively, to the factor. Other dominant signals of naphthalene diamine (m/z 159.102,  $\text{C}_{10}\text{H}_{11}\text{N}_2$ ) and methoxy benzopyranone (m/z 177.056,  $\text{C}_{10}\text{H}_9\text{O}_3$ ) relatively contribute about 34.5% and 44.45% to the factor. Naphthalene is present in ambient air due to emissions from the industries such as primary metal industries, chemical manufacturing industries, and pharmaceuticals (Preuss et al., 2003). Naphthalene is also used as an intermediate product in coal tar, dyes or inks, leather tanning and asphalt

**Formatted:** Font: (Default) Times New Roman, 10 pt

**Formatted:** Indent: First line: 0 cm

**Formatted:** Font: (Default) Times New Roman, 10 pt

**Formatted:** List Paragraph, Outline numbered + Level: 3 + Numbering Style: 1, 2, 3, ... + Start at: 1 + Alignment: Left + Aligned at: 0.63 cm + Indent at: 1.9

**Formatted:** Indent: First line: 0 cm

730 industries (Jia and Batterman, 2010). It is classified as a possible human carcinogen and precursor of atmospheric SOA (Jia and Batterman, 2010; Tang et al., 2020).

735 It is observed that there are very sharp peaks in the concentrations of [formaldehyde](#), ethanol, naphthalene, naphthalene diamine and benzopyrene in the high-resolution timeseries, as shown in supplementary Figure S6. This may be due to the influence of particular activity in near-by industries. A conglomerate of the industries is present in the southwest direction of the sampling site within and outside the city, as shown in Figure 1. The direction of the wind changes to the southwest during summers may have brought the high levels of naphthalene and its derivatives emitted from these industrial areas to the sampling site. The CWT graph also shows the strong influence of the source present in the southwest direction of the sampling site (supplementary Figure S3). A previous study has found that among the emitted OVOCs from sewage sludge, first-order OVOCs constituent ~60%, followed by high-order OVOCs (Haider et al., 2022).

740 Interestingly, there are three sewage treatment plants located near the sampling site. They may have [also](#) influenced the concentrations of OVOCs at the sampling site. The influence of factor contribution during summertime is probably due to the increased production of naphthalene, [formaldehyde](#), and ethanol from their local industrial sources and secondary formations at higher temperatures, as shown in the time series of the factors (supplementary Figure S7).

### 745 3.3. Correlation with AMS factors and other external factors

750 The timeseries of the five factors resolved from NMVOCs mass spectra are co-related with external measurements such as oxygenated organic aerosols (OOA), Black carbon (BC) concentrations, CAAQMS data (WD, WS, RH, Temp, NO, NO<sub>2</sub>, NO<sub>x</sub>, SO<sub>2</sub>, Ozone) as given in Figure 8. The VOC's traffic factor shows a temporal correlation (Pearson  $r^2 \sim 0.43$ ) with nitrogen oxides (NO<sub>x</sub>), which is also an indicator of vehicular emissions. This infers the NO<sub>x</sub> emissions along with NMVOCs from the vehicular fleet. Similarly, SFC 1 factor correlates with organics fraction of Nr-PM<sub>2.5</sub> (Org\_Hr), NO<sub>2</sub>\_Hr (inorganics NO<sub>3</sub> of Nr-PM<sub>2.5</sub>) and RH well with Pearson  $r^2 \sim 0.46, 0.53$ , and 0.47, respectively. The correlation coefficient between SFC 2 and black carbon concentrations is ~0.4. Volatile chemical products show good temporal co-relation with a solvent-based NMVOCs species, acetone, with Pearson  $r^2 \sim 0.6$ .

755 Figure 9 shows the scatter plots of individual VOC factors correlated with the most probable related sources, resolved after performing the PMF analysis on the mass spectra of the organic portion of NR-PM<sub>2.5</sub> (non-refractory PM<sub>2.5</sub>) measured by HR-ToF-AMS during the campaign. The detailed analysis and results of PMF of NR-PM<sub>2.5</sub> are given in other studies (Lalchandani et al., 2021; Talukdar et al., 2021; Tobler et al., 2020), beyond the scope of this paper. In brief, the organic aerosols (OA) mass spectra from HR-ToF-AMS were explained by 760 5-factors consisting of one hydrocarbon-like organic aerosols factor (AMS\_HOA), two solid fuel combustion factors (AMS\_SFC/BB& AMS\_SFC/OA), one more-oxidised oxygenated OA (AMS\_MO-OOA) and one low-oxidised oxygenated OA (AMS\_LO-OOA). [In this study, the traffic factor resolved from VOCs mass spectra has a good correlation \(Pearson  \$r^2 \sim 0.65\$ \) with the AMS\\_HOA](#), as shown in Figure 9 (a). This AMS\_HOA factor is characterised by aliphatic hydrocarbons, typically associated with traffic exhaust emissions (Lalchandani et al., 2021). It infers that vehicular exhaust is one of the common sources influencing the release of VOCs and primary OA. These VOCs and primary OA also exhibit similar diurnal solid variation, having sharp peaks during morning and evening hours during the rush hours, as shown in supplementary Figure S7.

770 The SFC factors resolved from organic mass spectra contained significant signals from unsaturated hydrocarbons, polyaromatic hydrocarbons, and oxygenated fragments (Lalchandani et al., 2021; Shukla et al., 2021). The AMS\_SFC/OA factor relates to the primary emissions from the combustion process of wood and paper, and biomass is influenced by a higher O/C (~0.878) ratio than the AMS\_SFC/BB O/C ratio (~0.268). The resolved factor from VOCs mass spectra related to biomass burning (SFC 1) shows a strong temporal correlation (Pearson  $r^2 \sim 0.85$ ) with AMS\_SFC/OA. Thus, we interpret SFC 1 as more related to conventional biomass burning at the site. The correlation of SFC 1 with organics Nr-PM<sub>2.5</sub> This argues that the domestic usage of biomass for cooking and other purposes is one of the leading factors for primary emissions of gas-phase (SFC 1) and particle-phase oxygenates (OOA). The factor SFC 2, derived from the VOC mass spectra, is more related (Pearson  $r^2 \sim 0.54$ ) to the AMS\_MO-OOA as shown in Figure 9 (e) and supplementary Figure S7. AMS\_MO-OOA is characterised by higher m/z 44 (CO<sub>2</sub>) and m/z 43 (C<sub>2</sub>H<sub>3</sub>O) fractions than the primary OA sources. This factor is comparatively more oxidised, having an O/C ratio of ~0.89 than AMS\_LO-OOA (O/C ratio ~0.62). We interpret that SFC 2 is influenced by fresh oxidation of primary biomass burning emissions.

775 Formatted: Not Highlight

780 Field Code Changed

### 3.4. OFP and SOA yield from individual sources

Formatted: Normal, No bullets or numbering

Based on the method explained in section 2.5, the ozone formation potential was calculated for each factor after considering the MIR values of NMVOCs species as given in supplementary Table S2. The relative contribution of each NMVOCs ions to the individual factor after PMF analysis is multiplied by the averaged individual concentration of the NMVOC species. The five highest contributor species to the ozone formation potential is toluene, followed by xylene, isoprene, and formaldehyde, and methyl cyclohexene. The distribution of individual sources to OFP is shown in Figure 10 (a). Toluene, xylene, and isoprene were found to be the highest contributor in terms of OFP in other Asian cities including Guangzhou, and Beijing also (Duan et al., 2008; Zhan et al., 2021; Zheng et al., 2009; Zhu et al., 2016). In the previous study in Delhi, it has also been noticed that contributions of aromatics (xylene and toluene) have substantial effect to the ozone formation potential (Tripathi et al., 2022). The traffic factor contributes maximum to the OFP among all the factors with 34.6%, followed by SFC1 (23.9%), then SFC 2(14.5%), SVOC (13.5%) and VCPs (13.5%).

Similarly, the contribution towards the formation of SOA is also estimated for each factor with SOA yield of individual NMVOCs ions as given in supplementary Table S3. The overall SOA yield is influenced by toluene, benzene, phenol, methyl furan, naphthalene, xylene, methyl furan, and trimethyl benzene. These compounds mostly belong to the aromatics and first-order oxygenates family. The measured SOA from HR-ToF-AMS may be considered as the sum of more-oxidised oxygenated OA factor (AMS MO-OOA) and one low-oxidised oxygenated OA (AMS LO-OOA) factor (Lalchandani et al., 2021). The five highest contributors to SOA formation potential were correlated with the measured SOA, in the supplementary figure S. The high-resolution time series shows the co-occurrence of high and low peaks of benzene, toluene, and xylene with measured SOA during the day and night hours. This shows the significant role of aromatic NMVOC species in the formation of SOA. The primary factors, Traffic and SFC 1, are the highest contributors to the SOA formation at with 28% and 27%, respectively, as shown in Figure 10 (b). These factors are ridden with the highest SOA formation contributing NMVOCs species. Previous studies have also found that aromatic hydrocarbons contributed more than 95% to the SOA formation potential in other Asian cities (J. Qin et al., 2021; Zhan et al., 2021). It was observed that the sources related to vehicular emissions (diesel and petrol driven vehicles), paddy stubble fire, and garbage fire emissions were most contributing factors for ozone formation potential in Mohali (Kumar et al., 2020). In the present study, the SVOC factor contributes 22% to the SOA formation, with maximum contribution from high-molecular oxygenated species. The SFC 2 and VCPs are less contributing towards the SOA formation.

In contrast, this sequence is not similar to the relative contribution of the sources according to their concentration (Figure 10 (c)). The source contributing to the highest concentration of NMVOCs is SFC 1, followed by traffic, SVOC, and VCPs. The lowest contributor is SFC 2. This comparison shows the importance of the source of NMVOCs towards SOA and ozone chemistry. The factor contributing the highest to the concentration of NMVOCs may not necessarily influence the ozone and SOA formation in the same way. These values are the estimates of potential for ozone and SOA formation and does not indicate the actual yields of ozone and SOA. This estimation method merely represents the complex behaviour of NMVOCs, NOx and solar radiation for producing tropospheric ozone and SOA. There are many NMVOCs species with unknown ozone and SOA yield values. It is needed to understand the chemical fates and pathways of many NMVOCs through mimicking real-time atmosphere in smog-chamber studies or through computational modelling studies. More research on this section is needed. More research on the section is needed. Nonetheless, other parameter including solar radiation, concentration of oxides of nitrogen also play key role in the formation of ozone in the troposphere. In reality, OFP and SOA do not provide complete information about how VOCs influence O3 and organic aerosol chemistry.

Ozone formation in Lucknow is more sensitive to NMVOCs concentrations than NOx, similar to other Asian cities. So, Decreasing VOCs/NOx ratio would help in reducing the secondary pollutants (O3 and SOA) as well. It is observed that vehicular emissions were the main source of aromatics (benzene, toluene, xylene). Therefore, strategies related to vehicular emission control should be implemented for the aromatics reduction (BTEX). Stringent implementation of policies and fuel-efficient standards related to vehicular emissions in Japan and South Korea have largely improved the air quality (13-17% reduction in NMVOCs) (Wang et al., 2014) (Wang et al., 2014 ACP). In the present study, one of the main keen observation was that toluene is the main contributor for both SOA and ozone production potential. This illustrates that targeting other sources of some NMVOCs (toluene, and xylene) as well will enhance its control. For example, paint solvents (source of ethylbenzene and

Formatted: Font: (Default) Times New Roman, Font color: Auto, English (United States)

Formatted: Not Highlight

Formatted: Not Highlight

Formatted: Font: (Default) Times New Roman, 10 pt, Font color: Auto, English (United States)

xylene) and printing products (source of toluene) were targeted in a city, Hong Kong where VOC content of 172 type of consumer products were prescribed by the respective government (Lyu et al., 2017) (Lyu et al., 2017). In the present study, other potential contributor species are found as methyl cyclohexeneformaldehyde (for ozone) and naphthalene (for SOA). These compounds are related to volatile chemical products, as found in the PMF analysis in Lucknow. This infers that the stringent policies related to solvent-based industries such as textile, automobile, paints, disinfectants is needed. Regulation and control of NMVOCs content in manufacturing and use of solvent-based products such as paints, disinfectants, fungicide, and insecticide should also be implemented. In China, end of pipe measures were implemented at various industries for control of NMVOCs such as refineries, plant oil extraction, gasoline storage and service stations, pharmacies, and crude oil storage and distribution (Wang et al., 2014). (Wang et al., 2014). It is also estimated that end-of pipe technologies and new energy saving policies in China would help in decreasing about one third of NMVOCs emissions (Zhang et al., 2020) (Zhang et al., 2020). Phenols and Furans, observed as one of the highest contributor to SOA formation potential, related to solid fuel combustion. This suggests the control of fossil fuel usage for residential energy, and crop-residue burning in the fields within and around the city, Lucknow. Firewood burning during heating period and domestic in-fields straw burning have substantially reduced emissions from biomass burning in China (Wu et al., 2020) (Wu et al., 2020). (Derwent et al., 2007) reported that reactivity-based VOC control measures might be more effective than mass-based regulations in terms of controlling ozone and secondary organic aerosol formation. The present study also suggests that the reduction of VOC especially from the vehicular emission is needed for the Abatement of ozone and SOA formation in urban areas."

**Formatted:** Font: (Default) Times New Roman, Font color: Auto, English (United States)

#### 4. Comparison with other Indian and Asian cities

Figure 11 represents mapped pie-chart to compare overall NMVOCs concentrations, and relative source contributions in different Asian and Indian cities. The earlier studies reported the total NMVOCs concentrations between 15-35 ppbv in different cities of China during winters (Hui et al., 2018; Wang et al., 2016, 2021a; Yang et al., 2018). The highest concentration of NMVOCs found in Wuhan city (~34.6 ppbv) with maximum contributions from alkanes and oxygenated VOCs (Hui et al., 2018). The relative composition of sources of NMVOCs found in Wuhan was Industrial/Solvent usage (29.9%), followed by traffic (24.4%), fuel evaporation (23.87%), biomass burning (19.3%) and biogenic (2.5%). The urban site in Beijing reported maximum contribution from secondary VOCs (54.6%), followed by biomass burning (24.4%) and traffic (21%) (Wang et al., 2021a) while the rural site in Beijing had significant contributions from biomass burning (37%) (Yang et al., 2018). Industrial and Traffic contributed similarly at the rural site in Beijing (~31.5%). The difference of source profiles and contributions in urban and rural areas inferred the need of different control strategies and policies in the country (Zhang et al., 2020). It is found that vehicular emissions and biomass burning sources contributes to NMVOCs concentrations (average ~21.5 ppbv) overall 50%, and 41%, respectively during summers, in a land locked urban city, Lhasa, Tibet (Guo et al., 2022) while Industrial/Solvent usage contributed 68% to NMVOCs (average ~33.7 ppbv) in Tokyo, Japan (Fukusaki et al., 2021b). It is interesting to note that near the coastal region in Hong Kong, 63.7% and 13.5 % NMVOCs contributions (average ~9.8 ppbv) are related to biomass burning and ship emissions (Tan et al., 2021). Despite various air pollution control strategies implemented for more than a decade, NMVOCs and O<sub>3</sub> concentrations did not decrease at significant levels in Hong Kong (Lyu et al., 2017). Previous study in Kathmandu (Sarkar et al., 2017), Nepal demonstrated that biomass co-fired brick kilns (29%) and traffic (28%) contributes to SOA production significantly. Other sources, such as Industrial/ Solvent-usage, biomass burning, and biogenic related emissions also dominated in the city.

**Formatted:** Font: (Default) Times New Roman, 12 pt, Bold

**Formatted:** Justified

Earlier source apportionment studies over the NMVOCs mass spectra conducted in Indian cities are limited to two cities in upper IGB region, Delhi (full year) and Mohali (summer). Comparing the urban and sub-urban site of Delhi found that vehicular emissions are dominant at both sites, relatively less contributions to NMVOCs at sub-urban region (36%) as compared to urban region (57%). Throughout the year, traffic emissions dominated the NMVOCs concentration (31%), with comparable contributions from biomass burning (28%), and secondary formations (31%) overall in Delhi. Mohali is located upwind of Delhi city, with maximum contributions from biomass burning (47%), followed by traffic (25%), and secondary formations (16%). The industrial source contributed about 5%, and

**Formatted:** Normal, Justified, No bullets or numbering

885 12% to NMVOCs concentrations in Delhi and Mohali, respectively. While in the present study, it is  
886 found that the solid fuel combustion related emissions majorly (41.3%) contributed to NMVOCs  
887 concentrations in Lucknow, located in the central IGB region. The traffic-related emissions (23.5%)  
888 and secondary formations (18.6%) are relatively less contributing to NMVOCs as compared to upper  
889 IGB region cities (Delhi and Mohali). Moreover, the volatile chemical products emitted more during  
890 summer period in Lucknow than compared to Delhi and Mohali. Solid fuel combustion sources aided  
891 concentrations of NMVOCs in both Mohali and Lucknow significantly. This may be due to both cities  
892 are located downwind of widespread area of agricultural fields. Both of these cities observed relatively  
893 less formations of secondary volatile organic compounds, suggested the dominance of fresh emissions  
894 than aged compounds in the air mass. Overall, the ambient concentrations of NMVOCs in Indian cities  
895 majorly influenced by emissions from solid fuel combustion, vehicular related emissions, secondary  
896 formations, and industrial sources. This suggested the need of control measures, and policies  
897 implemented for specific sources country-wide and specific to city.

Formatted: Not Highlight

900 **Conclusion**

**5. Conclusion**

905 This study investigated the high time-resolved chemical characterisation of NMVOCs in Lucknow between December 2020 and May 2021. The mass spectra of the NMVOCs were used to perform source apportionment and study the diurnal variations. The individual species were identified as per their chemical formulae and exhibit large temporal fluctuations. The highest NMVOCs concentrations during winters were due to their increased emissions from solid fuel combustion and stagnant conditions due to less mixing height. The warmer period between April and May showed the influence of high photochemical activity and regional transport. The major industries observed to be present in the southwest direction of the sampling site, which may be responsible for elevated volatile chemical products during summer. The 910 five major factors resolved from source apportionment were a traffic factor, two solid fuel combustion factors, secondary VOCs, and VCPs. The primary sources, such as traffic factor and solid fuel combustion, exhibited a stronger correlation with organic aerosol resolved factors, infers their common time of origin from similar sources. The traffic factor had a similar profile found in Delhi, which suggested a similar vehicular pattern and fuel composition in different urban centers of the IGB region of India. The 915 biomass burning factors in Lucknow had distinct profiles from Delhi due to different cooking or domestic fuel consumption and cropping patterns. Moreover, the regional transport of secondary volatile organic compounds was also observed in the back-trajectory analysis. The VCPs factor significantly contributes to The primary first-order oxygenates most contributed to VCPs factor, while the secondary VOCs factor had contributions from second and third-order oxygenates. The highest contributing factor towards the 920 NMVOCs emissions in Lucknow was found to be solid fuel combustion (SFC 1) and traffic. The PTR-ToF-MS resolved source factors of NMVOCs were correlated with HR-ToF-AMS resolved factors,  $\text{Nr-PM}_{2.5}$  (organics and inorganics), and supporting measurements (BC, NO<sub>x</sub>, SO<sub>2</sub>, O<sub>3</sub>) to analyze their common 925 sources and diurnal patterns. The Ozone and SOA formation potential from individual NMVOCs species and sources were also estimated using MIR and SOA yield values-based methods, respectively. There is a scope of improving these estimates as these values represented the potential for formation of SOA and O<sub>3</sub>, not the actual yields. It is found that a few of the NMVOCs species are significantly responsible for 930 secondary pollutant formations. Stringent policies and control actions regarding aromatics (benzene, toluene, xylene, and naphthalene) and oxygenates (phenol, furans, and formaldehyde) could reduce the NMVOCs emissions drastically. The sources which were potentially contributing to SOA and ozone 935 formations identified as traffic, SFC and VCPs. Further control measures and end to pipe technologies to reduce emissions from solvent-based industries, consumer products, residential and domestic biomass burning and vehicular fleet are required to mitigate the health and environmental impacts of NMVOCs and secondary pollutants. The formation of ozone and SOA is driven by the oxidation. The results of this study suggest that in order to improve air quality in urban regions of India, particularly the Indo-Gangetic Plain, a comprehensive measurement of VOCs is necessary to characterize their emission sources and understand their photochemical processes.

Formatted: Indent: First line: 0 cm

Formatted: Font: (Default) Times New Roman, 10 pt

Formatted: Indent: First line: 0 cm

Formatted: Font: (Default) Times New Roman, 12 pt, Bold

Formatted: Left

Formatted: List Paragraph, Justified, Indent: Left: 0.18 cm, Right: 0.61 cm, Space Before: 8.25 pt, No widow/orphan control, Don't adjust space between Latin and Asian text, Don't adjust space between Asian text and numbers, Tab stops: 0.69 cm, Left

Formatted: Subscript

Formatted: Subscript

Formatted: Font: (Default) Times New Roman, 10 pt, Font color: Auto, English (United States)

940

of NMVOCs. The NMVOCs and NO<sub>x</sub> derive from the formation of ozone and SOA, but there is limited knowledge of their complex relationship. However, ozone and SOA formations are estimated using available studies in the best way possible. There is a scope for improving these values in further studies. It is interesting to note that the primary factors, Traffic and SFC 1, are crucial in Lucknow city for NMVOCs emissions and ozone and SOA formation. This work highlights that the NMVOCs sources are highly influenced by local emissions, meteorology, city planning and implementation of the policies in the IGB region. Further studies focusing on VOCs-secondary organic aerosol interactions would help identify the gas-particle partitioning, ageing and transport of pollution in the region.

Formatted: Indent: First line: 0 cm

945

#### 4.6. Data availability

Formatted: Font: 12 pt

The data is available on the request with corresponding author.

950

#### 5.7. Author Contribution

Formatted: Font: 12 pt

955

**Vaishali Jain:** Conceptualization, data curation, Methodology, Software, Validation, Formal analysis, Investigation, Writing– original draft, Writing– review & editing, Visualization **Sachchida N. Tripathi:** Conceptualization, Writing– review & editing, Supervision, Project administration, Funding acquisition **Nidhi Tripathi:** Investigation, Data curation, Validation, Writing– review & editing, **Mansi Gupta:** Investigation, Data curation, Validation, Writing– review & editing, **Lokesh K. Sahu:** Resources, Methodology, Validation, Writing– review & editing **Sreenivas Gaddamidi:** Investigation, Data curation, Validation, **Ashutosh K. Shukla:** Validation, Writing– review & editing, **Vishnu Murari:** Formal analysis, Validation, Writing– review & editing, **Andre S.H. Prevot:** Methodology, Validation, Writing– review & editing.

960

#### 6.8. Competing interests

Formatted: Font: 12 pt

The authors declare that they have no known competing financial interests or personal relationships that could have appeared to influence the work reported in this paper.

965

#### 9 Acknowledgements

Formatted: Numbered + Level: 1 + Numbering Style: 1, 2, 3, ... + Start at: 9 + Alignment: Left + Aligned at: 0.63 cm + Indent at: 1.27 cm

970

LKS, NT and MG acknowledge Prof. Anil Bhardwaj, Director, Physical Research Laboratory (PRL), Ahmedabad, India, for the support and permission to deploy PTR-TOF-MS during the experimental campaign. SNT and VJ gratefully acknowledge the financial support provided by the Swiss Agency for Development and Cooperation, Switzerland, to conduct this research under project no. 7F-10093.01.04 (contract no. 81062452). SNT also acknowledges the support from Duke University, Office of Research Support, Subaward no. 349-0685. The authors would like to acknowledge the support from UPPCB (Uttar Pradesh Pollution Control Board) for the set-up of the campaign site. The authors would also like to acknowledge the support of PSI and Centre of Excellence (ATMAN) approved by the office of the Principal Scientific Officer to the Government of India. The CoE is supported by philanthropies including Bloomberg Philanthropies, the Children's Investment Fund Foundation (CIFF), the Open Philanthropy and the Clean Air Fund.

975

#### References

Formatted: No bullets or numbering

980

Anenberg, S. C., Henze, D. K., Tinney, V., Kinney, P. L., Raich, W., Fann, N., Malley, C. S., Roman, H., Lamsal, L., Duncan, B., Martin, R. V., van Donkelaar, A., Brauer, M., Doherty, R., Jonson, J. E., Davila, Y., Sudo, K., and Kuylenstierna, J. C. I.: Estimates of the Global Burden of Ambient PM<sub>2.5</sub>, Ozone, and NO<sub>2</sub> on Asthma Incidence and Emergency Room Visits, *Environ Health Perspect*, 126, 107004, <https://doi.org/10.1289/EHP3766>, 2018.

Atkinson\*, R.: Atmospheric chemistry of VOCs and NO<sub>x</sub>, *Sens Actuators B Chem*, 2000.

Atkinson, R. and Arey, J.: Atmospheric Degradation of Volatile Organic Compounds, *Chem Rev*, 103, 4605–4638, <https://doi.org/10.1021/cr0206420>, 2003.

Atkinson, R., Baulch, D. L., Cox, R. A., Crowley, J. N., Hampson, R. F., Hynes, R. G., Jenkin, M. E., Rossi, M. J., and Troe, J.: Evaluated kinetic and photochemical data for atmospheric chemistry: Volume 1 – gas phase reactions of Ox, HO<sub>x</sub>, NO<sub>x</sub> and SO<sub>x</sub> species, *Atmos Chem Phys*, 4, 1461–1738, <https://doi.org/10.5194/acp-4-1461-2004>, 2004.

[Brief Industrial Profile of District Lucknow, Uttar Pradesh, Lucknow, 1–21 pp., 2018.](#)

985 [Balakrishnan, K., Chen, G., Brauer, M., and Chow, J.: IARC Monographs on the Evaluation of Carcinogenic Risks to Humans: Outdoor Air Pollution, IARC , WHO, 1–656 pp., 2015.](#)

[Baudic, A., Gros, V., Sauvage, S., Locoge, N., Sanchez, O., Sarda-Estève, R., Kalogridis, C., Petit, J. E., Bonnaire, N., Baisnée, D., Favez, O., Albinet, A., Sciare, J., and Bonsang, B.: Seasonal variability and source apportionment of volatile organic compounds \(VOCs\) in the Paris megacity \(France\), \*Atmos Chem Phys\*, 16, 11961–11989, <https://doi.org/10.5194/acp-16-11961-2016>, 2016.](#)

990 [Blake, R. S., Whyte, C., Hughes, C. O., Ellis, A. M., and Monks, P. S.: Demonstration of proton-transfer reaction time-of-flight mass spectrometry for real-time analysis of trace volatile organic compounds, \*Anal Chem\*, 76, 3841–3845, <https://doi.org/10.1021/ac0498260>, 2004.](#)

[Blake, R. S., Monks, P. S., and Ellis, A. M.: Proton-transfer reaction mass spectrometry, \*Chem Rev\*, 109, 861–896, <https://doi.org/10.1021/cr800364q>, 2009.](#)

995 [Brilli, F., Gioli, B., Ciccioli, P., Zona, D., Loreto, F., Janssens, I. A., and Ceulemans, R.: Proton Transfer Reaction Time-of-Flight Mass Spectrometric \(PTR-TOF-MS\) determination of volatile organic compounds \(VOCs\) emitted from a biomass fire developed under stable nocturnal conditions, \*Atmos Environ\*, 97, 54–67, <https://doi.org/10.1016/j.atmosenv.2014.08.007>, 2014.](#)

1000 [Bruns, E. A., Slowik, J. G., El Haddad, I., Kilic, D., Klein, F., Dommen, J., Temime-Roussel, B., Marchand, N., Baltensperger, U., and Prévôt, A. S. H.: Characterization of gas-phase organics using proton transfer reaction time-of-flight mass spectrometry: Fresh and aged residential wood combustion emissions, \*Atmos Chem Phys\*, 17, 705–720, <https://doi.org/10.5194/acp-17-705-2017>, 2017.](#)

1005 [Burnett, R. T., Arden Pope, C., Ezzati, M., Olives, C., Lim, S. S., Mehta, S., Shin, H. H., Singh, G., Hubbell, B., Brauer, M., Ross Anderson, H., Smith, K. R., Balmes, J. R., Bruce, N. G., Kan, H., Laden, F., Prüss-Ustün, A., Turner, M. C., Gapstur, S. M., Diver, W. R., and Cohen, A.: An integrated risk function for estimating the global burden of disease attributable to ambient fine particulate matter exposure, \*Environ Health Perspect\*, 122, 397–403, <https://doi.org/10.1289/ehp.1307049>, 2014.](#)

1010 [Canonaco, F., Crippa, M., Slowik, J. G., Baltensperger, U., and Prévôt, A. S. H.: SoFi, an IGOR-based interface for the efficient use of the generalized multilinear engine \(ME-2\) for the source apportionment: ME-2 application to aerosol mass spectrometer data, \*Atmos Meas Tech\*, 6, 3649–3661, <https://doi.org/10.5194/amt-6-3649-2013>, 2013.](#)

1015 [Canonaco, F., Tobler, A., Chen, G., Sosedova, Y., Gates Slowik, J., Bozzetti, C., Rudolf Daellenbach, K., El Haddad, I., Crippa, M., Huang, R. J., Furger, M., Baltensperger, U., and Prévôt, A. S. H.: A new method for long-term source apportionment with time-dependent factor profiles and uncertainty assessment using SoFi Pro: Application to 1 year of organic aerosol data, \*Atmos Meas Tech\*, 14, 923–943, <https://doi.org/10.5194/amt-14-923-2021>, 2021.](#)

[Cao, X., Yao, Z., Shen, X., Ye, Y., and Jiang, X.: On-road emission characteristics of VOCs from light-duty gasoline vehicles in Beijing, China, \*Atmos Environ\*, 124, 146–155, <https://doi.org/10.1016/j.atmosenv.2015.06.019>, 2016.](#)

1020 [Captain, I., Cazier, F., Nouali, H., Mercier, A., Déchaux, J. C., Nollet, V., Joumard, R., André, J. M., and Vidon, R.: Emissions of unregulated pollutants from European gasoline and diesel passenger cars, \*Atmos Environ\*, 40, 5954–5966, <https://doi.org/10.1016/j.atmosenv.2005.12.049>, 2006.](#)

1025 [Cappellin, L., Karl, T., Probst, M., Ismailova, O., Winkler, P. M., Soukoulis, C., Aprea, E., Märk, T. D., Gasperi, F., and Biasioli, F.: On quantitative determination of volatile organic compound concentrations using proton transfer reaction time-of-flight mass spectrometry, \*Environ Sci Technol\*, 46, 2283–2290, <https://doi.org/10.1021/es203985t>, 2012.](#)

[Carter, W.: Updated maximum incremental reactivity scale and hydrocarbon bin reactivities for regulatory applications, 2010.](#)

1030 Carter, W. P. L.: Development of ozone reactivity scales for volatile organic compounds, *J Air Waste Manage Assoc.*, 44, 881–899, <https://doi.org/10.1080/1073161x.1994.10467290>, 1994a.

1035 Carter, W. P. L.: Reactivity Estimates for Selected consumer product compounds, 2008.

Chameides, W. L., Fehsenfeld, F., Rodgers, M. O., Cardelino, C., Martinez, J., Parrish, D., Lonneman, W., Lawson, D. R., Rasmussen, R. A., Zimmerman, P., Greenberg, J., Middleton, P., and Wang, T.: Ozone precursor relationships in the ambient atmosphere, *J Geophys Res.*, 97, 6037–6055, <https://doi.org/10.1029/91JD03014>, 1992.

1040 Chattopadhyay, G., Samanta, G., Chatterjee, S., and Chakraborti, D.: Determination of benzene, toluene and xylene in ambient air of calcutta for three years during winter, *Environmental Technology (United Kingdom)*, 18, 211–218, <https://doi.org/10.1080/09593331808616529>, 1997.

1045 Chauhan, S. K., Saini, N., and Yadav, V. B.: Recent Trends of Volatile Organic Compounds in Ambient Air & Its Health Impacts : a Review, *International Journal For Technological Research In Engineering*, 1, 667–678, 2014.

Coggon, M. M., Lim, C. Y., Koss, A. R., Sekimoto, K., Yuan, B., Gilman, J. B., Hagan, D. H., Selimovic, V., Zarzana, K. J., Brown, S. S., M Roberts, J., Müller, M., Yokelson, R., Wisthaler, A., Krechmer, J. E., Jimenez, J. L., Cappa, C., Kroll, J. H., De Gouw, J., and Warneke, C.: OH chemistry of non-methane organic gases (NMOGs) emitted from laboratory and ambient biomass burning smoke: Evaluating the influence of furans and oxygenated aromatics on ozone and secondary NMOG formation, *Atmos Chem Phys.*, 19, 14875–14899, <https://doi.org/10.5194/acp-19-14875-2019>, 2019.

1050 Davison, A. C. and Hinkley, D. V.: *Bootstrap Methods and their Application*, Cambridge University Press, <https://doi.org/10.1017/CBO9780511802843>, 1997.

Decarlo, P. F., Kimmel, J. R., Trimborn, A., Northway, M. J., Jayne, J. T., Aiken, A. C., Gonin, M., Fuhrer, K., Horvath, T., Docherty, K. S., Worsnop, D. R., and Jimenez, J. L.: Field-Deployable, High-Resolution, Time-of-Flight Aerosol Mass Spectrometer, *Anal Chem.*, 78, 8281–8289, <https://doi.org/10.1029/2001JD001213>.Analytical, 2006.

1055 Derwent, R. G., Jenkin, M. E., Passant, N. R., and Pilling, M. J.: Reactivity-based strategies for photochemical ozone control in Europe, *Environ Sci Policy*, 10, 445–453, <https://doi.org/10.1016/j.envsci.2007.01.005>, 2007.

Drinovec, L., Močnik, G., Zotter, P., Prévôt, A. S. H., Ruckstuhl, C., Coz, E., Rupakheti, M., Sciare, J., Müller, T., Wiedensohler, A., and Hansen, A. D. A.: The “dual-spot” Aethalometer: An improved measurement of aerosol black carbon with real-time loading compensation, *Atmos Meas Tech*, 8, 1965–1979, <https://doi.org/10.5194/amt-8-1965-2015>, 2015.

1060 Drinovec, L., Gregoric, A., Zotter, P., Wolf, R., Anne Bruns, E., Bruns, E. A., Prevot, A. S. H., Favez, O., Sciare, J., Arnold, I. J., Chakrabarty, R. K., Moosmüller, H., Filep, A., and Močnik, G.: The filter-loading effect by ambient aerosols in filter absorption photometers depends on the coating of the sampled particles, *Atmos Meas Tech*, 10, 1043–1059, <https://doi.org/10.5194/amt-10-1043-2017>, 2017.

1065 Duan, J., Tan, J., Yang, L., Wu, S., and Hao, J.: Concentration, sources and ozone formation potential of volatile organic compounds (VOCs) during ozone episode in Beijing, *Atmos Res.*, 88, 25–35, <https://doi.org/10.1016/j.atmosres.2007.09.004>, 2008.

Fukusaki, Y., Kousa, Y., Umehara, M., Ishida, M., Sato, R., Otagiri, K., Hoshi, J., Nudejima, C., Takahashi, K., and Nakai, S.: Source region identification and source apportionment of volatile organic compounds in the Tokyo Bay coastal area, Japan, *Atmos Environ X*, 9, 100103, <https://doi.org/10.1016/j.aeaoa.2021.100103>, 2021a.

1070 Fukusaki, Y., Kousa, Y., Umehara, M., Ishida, M., Sato, R., Otagiri, K., Hoshi, J., Nudejima, C., Takahashi, K., and Nakai, S.: Source region identification and source apportionment of volatile organic compounds in the Tokyo Bay coastal area, Japan, *Atmos Environ X*, 9, 100103, <https://doi.org/10.1016/j.aeaoa.2021.100103>, 2021b.

1075 Garg, A., Gupta, N. C., and Tyagi, S. K.: Study of seasonal and spatial variability among benzene, toluene, and p-Xylene (BTp-X) in ambient air of Delhi, India, *Pollution*, 5, 135–146, <https://doi.org/10.22059/poll.2018.260934.469>, 2019.

Gilman, J. B., Lerner, B. M., Kuster, W. C., and De Gouw, J. A.: Source signature of volatile organic compounds from oil and natural gas operations in northeastern Colorado, Environ Sci Technol, 47, 1297–1305, <https://doi.org/10.1021/es304119a>, 2013.

1080 de Gouw, J. A., Middlebrook, A. M., Warneke, C., Goldan, P. D., Kuster, W. C., Roberts, J. M., Fehsenfeld, F. C., Worsnop, D. R., Canagaratna, M. R., Pszenny, A. A. P., Keene, W. C., Marchewka, M., Bertman, S. B., and Bates, T. S.: Budget of organic carbon in a polluted atmosphere: Results from the New England Air Quality Study in 2002, Journal of Geophysical Research D: Atmospheres, 110, 1–22, <https://doi.org/10.1029/2004JD005623>, 2005.

1085 Government of India, M. of R. T. and H. T. R. wing: Road Transport Year Book (2016-17), 2019.

1090 Graus, M., Müller, M., and Hansel, A.: High resolution PTR-TOF: Quantification and Formula Confirmation of VOC in Real Time, J Am Soc Mass Spectrom, 21, 1037–1044, <https://doi.org/10.1016/j.jasms.2010.02.006>, 2010.

1095 Guo, S., Wang, Y., Zhang, T., Ma, Z., Ye, C., Lin, W., Yang Zong, D. J., and Yang Zong, B. M.: Volatile organic compounds in urban Lhasa: variations, sources, and potential risks, Front Environ Sci, 10, 1–16, <https://doi.org/10.3389/fenvs.2022.941100>, 2022.

1100 Haider, K. M., Lafouge, F., Carpentier, Y., Houot, S., Petitprez, D., Loubet, B., Focsa, C., and Ciuraru, R.: Chemical identification and quantification of volatile organic compounds emitted by sewage sludge, Science of the Total Environment, 838, <https://doi.org/10.1016/j.scitotenv.2022.155948>, 2022.

1105 Hallquist, M., Wenger, J. C., Baltensperger, U., Rudich, Y., Simpson, D., Claeys, M., Dommen, J., Donahue, N. M., George, C., Goldstein, A. H., Hamilton, J. F., Herrmann, H., Hoffmann, T., Iinuma, Y., Jang, M., Jenkin, M. E., Jimenez, J. L., Kiendler-Scharr, A., Maenhaut, W., McFiggans, G., Mentel, T. F., Monod, A., Prévôt, A. S. H., Seinfeld, J. H., Surratt, J. D., Szmigielski, R., and Wildt, J.: The formation, properties and impact of secondary organic aerosol: Current and emerging issues, Atmos Chem Phys, 9, 5155–5236, <https://doi.org/10.5194/acp-9-5155-2009>, 2009.

1110 Hansel, A., Jordan, A., Warneke, C., Holzinger, R., Wisthaler, A., and Lindinger, W.: Proton-transfer-reaction mass spectrometry (PTR-MS): On-line monitoring of volatile organic compounds at volume mixing ratios of a few pptv, Plasma Sources Sci Technol, 8, 332–336, <https://doi.org/10.1088/0963-0252/8/2/314>, 1999.

1115 Harrison, M. A. J., Barra, S., Borghesi, D., Vione, D., Arsene, C., and Iulian Olariu, R.: Nitrated phenols in the atmosphere: A review, Atmos Environ, 39, 231–248, <https://doi.org/10.1016/j.atmosenv.2004.09.044>, 2005.

1120 Heald, C. L., Henze, D. K., Horowitz, L. W., Feddema, J., Lamarque, J. F., Guenther, A., Hess, P. G., Vitt, F., Seinfeld, J. H., Godstein, A. H., and Fung, I.: Predicted change in global secondary organic aerosol concentrations in response to future climate, emissions, and land use change, Journal of Geophysical Research Atmospheres, 113, 1–16, <https://doi.org/10.1029/2007JD009092>, 2008.

Holzinger, R., Wameke, C., Hansel, A., Jordan, A., Lindinger, W., Scharffe, D. H., Schade, G., and Crutzen, P. J.: Biomass burning as a source of formaldehyde, acetaldehyde, methanol, acetone, acetonitrile, and hydrogen cyanide, Geophys Res Lett, 26, 1161–1164, <https://doi.org/10.1029/1999GL900156>, 1999.

Hoque, R. R., Khillare, P. S., Agarwal, T., Shridhar, V., and Balachandran, S.: Spatial and temporal variation of BTEX in the urban atmosphere of Delhi, India, Science of the Total Environment, 392, 30–40, <https://doi.org/10.1016/j.scitotenv.2007.08.036>, 2008.

1125 Hui, L., Liu, X., Tan, Q., Feng, M., An, J., Ou, Y., Zhang, Y., and Jiang, M.: Characteristics, source apportionment and contribution of VOCs to ozone formation in Wuhan, Central China, Atmos Environ, 192, 55–71, <https://doi.org/10.1016/j.atmosenv.2018.08.042>, 2018.

Jain, V., Tripathi, S. N., Tripathi, N., Sahu, L. K., Gaddamidi, S., Shukla, A. K., Bhattu, D., and Ganguly, D.: Seasonal variability and source apportionment of non-methane VOCs using PTR-TOF-MS measurements in Delhi, India, Atmos Environ, 283, 119163, <https://doi.org/10.1016/j.atmosenv.2022.119163>, 2022.

1130 Jang, M., Czoschke, N. M., Lee, S., and Kamens, R. M.: Heterogeneous atmospheric aerosol production by acid-catalyzed particle-phase reactions, Science (1979), 298, 814–817, <https://doi.org/10.1126/science.1075798>, 2002.

1125 Jayne, J. T., Worsnop, D. R., Kolb, C. E., Leard, D., Davidovits, P., Zhang, X., and Smith, K. A.: Aerosol mass spectrometer for size and composition analysis of submicron particles, *J Aerosol Sci.*, 29, 49–70, [https://doi.org/10.1016/S0021-8502\(98\)00158-X](https://doi.org/10.1016/S0021-8502(98)00158-X), 1998.

1130 Jayne, J. T., Leard, D. C., Zhang, X., Davidovits, P., Smith, K. A., Kolb, C. E., and Worsnop, D. R.: Development of an aerosol mass spectrometer for size and composition analysis of submicron particles, *Aerosol Science and Technology*, 33, 49–70, <https://doi.org/10.1080/027868200410840>, 2000.

1135 Jia, C. and Batterman, S.: A critical review of naphthalene sources and exposures relevant to indoor and outdoor air, *Int J Environ Res Public Health*, 7, 2903–2939, <https://doi.org/10.3390/ijerph7072903>, 2010.

1140 Jordan, A., Haidacher, S., Hanel, G., Hartungen, E., Märk, L., Seehauser, H., Schottkowsky, R., Sulzer, P., and Märk, T. D.: A high resolution and high sensitivity proton-transfer-reaction time-of-flight mass spectrometer (PTR-TOF-MS), *Int J Mass Spectrom.*, 286, 122–128, <https://doi.org/10.1016/j.ijms.2009.07.005>, 2009.

1145 Kerminen, V. M., Lihavainen, H., Komppula, M., Viisanen, Y., and Kulmala, M.: Direct observational evidence linking atmospheric aerosol formation and cloud droplet activation, *Geophys. Res. Lett.*, 32, 1–4, <https://doi.org/10.1029/2005GL023130>, 2005.

Kroll, J. H., Ng, N. L., Murphy, S. M., Flagan, R. C., and Seinfeld, J. H.: Secondary organic aerosol formation from isoprene photooxidation, *Environ. Sci. Technol.*, 40, 1869–1877, <https://doi.org/10.1021/es0524301>, 2006.

1150 Kumar, A., Sinha, V., Shabin, M., Hakkim, H., Bonsang, B., and Gros, V.: Non-methane hydrocarbon (NMHC) fingerprints of major urban and agricultural emission sources for use in source apportionment studies, *Atmos. Chem. Phys.*, 20, 12133–12152, <https://doi.org/10.5194/acp-20-12133-2020>, 2020.

1155 Laaksonen, A., Hamed, A., Joutsensaari, J., Hiltunen, L., Cavalli, F., Junkermann, W., Asmi, A., Fuzzi, S., and Facchini, M. C.: Cloud condensation nucleus production from nucleation events at a highly polluted region, *Geophys. Res. Lett.*, 32, 1–4, <https://doi.org/10.1029/2004GL022092>, 2005.

1160 Lalchandani, V., Kumar, V., Tobler, A., M. Thamban, N., Mishra, S., Slowik, J. G., Bhattu, D., Rai, P., Satish, R., Ganguly, D., Tiwari, S., Rastogi, N., Tiwari, S., Moćnik, G., Prévôt, A. S. H., and Tripathi, S. N.: Real-time characterization and source apportionment of fine particulate matter in the Delhi megacity area during late winter, *Science of the Total Environment*, 770, <https://doi.org/10.1016/j.scitotenv.2021.145324>, 2021.

Lalchandani, V., Srivastava, D., Dave, J., Mishra, S., Tripathi, N., Shukla, A. K., Sahu, R., Thamban, N. M., Gaddamidi, S., Dixit, K., Ganguly, D., Tiwari, S., Srivastava, A. K., Sahu, L., Rastogi, N., Gargava, P., and Tripathi, S. N.: Effect of Biomass Burning on PM<sub>2.5</sub> Composition and Secondary Aerosol Formation During Post-Monsoon and Winter Haze Episodes in Delhi, *Journal of Geophysical Research: Atmospheres*, 127, 1–21, <https://doi.org/10.1029/2021JD035232>, 2022.

1165 Laskin, A., Smith, J. S., and Laskin, J.: Molecular characterization of nitrogen-containing organic compounds in biomass burning aerosols using high-resolution mass spectrometry, *Environ. Sci. Technol.*, 43, 3764–3771, <https://doi.org/10.1021/es803456n>, 2009.

Lawrence, A. and Fatima, N.: Urban air pollution & its assessment in Lucknow City - The second largest city of North India, *Science of the Total Environment*, 488–489, 447–455, <https://doi.org/10.1016/j.scitotenv.2013.10.106>, 2014.

Lee, A., Goldstein, A. H., Keywood, M. D., Gao, S., Ng, N. L., Varutbangkul, V., Bahreini, R., Flagan, R. C., and Seinfeld, J. H.: Gas-phase products and secondary aerosol yields from the ozonolysis of ten different terpenes, *Journal of Geophysical Research Atmospheres*, 111, <https://doi.org/10.1029/2005JD006437>, 2006a.

Lee, A., Goldstein, A. H., Kroll, J. H., Ng, N. L., Varutbangkul, V., Flagan, R. C., and Seinfeld, J. H.: Gas-phase products and secondary aerosol yields from the photooxidation of 16 different terpenes, *Journal of Geophysical Research Atmospheres*, 111, <https://doi.org/10.1029/2006JD007050>, 2006b.

Li, Y. J., Huang, D. D., Cheung, H. Y., Lee, A. K. Y., and Chan, C. K.: Aqueous-phase photochemical oxidation and direct photolysis of vanillin - A model compound of methoxy phenols from biomass burning, *Atmos. Chem. Phys.*, 14, 2871–2885, <https://doi.org/10.5194/acp-14-2871-2014>, 2014.

1170 [Lyu, X. P., Zeng, L. W., Guo, H., Simpson, I. J., Ling, Z. H., Wang, Y., Murray, F., Louie, P. K. K., Saunders, S. M., Lam, S. H. M., and Blake, D. R.: Evaluation of the effectiveness of air pollution control measures in Hong Kong, Environmental Pollution, 220, 87–94, <https://doi.org/10.1016/j.envpol.2016.09.025>, 2017.](https://doi.org/10.1016/j.envpol.2016.09.025)

1175 [Majumdar, D., Mukherjee, A. K., and Sen, S.: BTEX in Ambient Air of a Metropolitan City, J Environ Prot \(Irvine, Calif\), 02, 11–20, <https://doi.org/10.4236/jep.2011.21002>, 2011.](https://doi.org/10.4236/jep.2011.21002)

1180 [Majumdar \(neé Som\), D., Dutta, C., Mukherjee, A. K., and Sen, S.: Source apportionment of VOCs at the petrol pumps in Kolkata, India: exposure of workers and assessment of associated health risk, Transp Res D Transp Environ, 13, 524–530, <https://doi.org/10.1016/j.trd.2008.09.011>, 2008.](https://doi.org/10.1016/j.trd.2008.09.011)

1185 [Markandeya, Verma, P. K., Mishra, V., Singh, N. K., Shukla, S. P., and Mohan, D.: Spatio-temporal assessment of ambient air quality, their health effects and improvement during COVID-19 lockdown in one of the most polluted cities of India, Environmental Science and Pollution Research, 28, 10536–10551, <https://doi.org/10.1007/s11356-020-11248-3>, 2021.](https://doi.org/10.1007/s11356-020-11248-3)

1190 [Mohr, C., Lopez-Hilfiker, F. D., Zotter, P., Prévoit, A. S. H., Xu, L., Ng, N. L., Herndon, S. C., Williams, L. R., Franklin, J. P., Zahniser, M. S., Worsnop, D. R., Knighton, W. B., Aiken, A. C., Gorkowski, K. J., Dubey, M. K., Allan, J. D., and Thornton, J. A.: Contribution of nitrated phenols to wood burning brown carbon light absorption in the United Kingdom during winter time, Environ Sci Technol, 47, 6316–6324, <https://doi.org/10.1021/es400683v>, 2013.](https://doi.org/10.1021/es400683v)

1195 [Monks, P. S., Granier, C., Fuzzi, S., Stohl, A., Williams, M. L., Akimoto, H., Amann, M., Baklanov, A., Baltensperger, U., Bey, I., Blake, N., Blake, R. S., Carslaw, K., Cooper, O. R., Dentener, F., Fowler, D., Fratou, E., Frost, G. J., Generoso, S., Ginoux, P., Grewe, V., Guenther, A., Hansson, H. C., Henne, S., Hjorth, J., Hofzumahaus, A., Huntrieser, H., Isaksen, I. S. A., Jenkins, M. E., Kaiser, J., Kanakidou, M., Klimont, Z., Kulmala, M., Laj, P., Lawrence, M. G., Lee, J. D., Liousse, C., Maione, M., McFiggans, G., Metzger, A., Mieville, A., Moussiopoulos, N., Orlando, J. J., O'Dowd, C. D., Palmer, P. I., Parrish, D. D., Petzold, A., Platt, U., Pöschl, U., Prévôt, A. S. H., Reeves, C. E., Reimann, S., Rudich, Y., Sellegri, K., Steinbrecher, R., Simpson, D., ten Brink, H., Theloke, J., van der Werf, G. R., Vautard, R., Vestreng, V., Vlachokostas, C., and von Glasow, R.: Atmospheric composition change - global and regional air quality, Atmos Environ, 43, 5268–5350, <https://doi.org/10.1016/j.atmosenv.2009.08.021>, 2009.](https://doi.org/10.1016/j.atmosenv.2009.08.021)

1200 [Monks, P. S., Archibald, A. T., Colette, A., Cooper, O., Coyle, M., Derwent, R., Fowler, D., Granier, C., Law, K. S., Mills, G. E., Stevenson, D. S., Tarasova, O., Thouret, V., von Schneidemesser, E., Sommariva, R., Wild, O., and Williams, M. L.: Tropospheric ozone and its precursors from the urban to the global scale from air quality to short-lived climate forcer, Atmos Chem Phys, 15, 8889–8973, <https://doi.org/10.5194/acp-15-8889-2015>, 2015.](https://doi.org/10.5194/acp-15-8889-2015)

1205 [Müller, M., Graus, M., Wisthaler, A., Hansel, A., Metzger, A., Dommen, J., and Baltensperger, U.: Analysis of high mass resolution PTR-TOF mass spectra from 1,3,5-trimethylbenzene \(TMB\) environmental chamber experiments, Atmos Chem Phys, 12, 829–843, <https://doi.org/10.5194/acp-12-829-2012>, 2012.](https://doi.org/10.5194/acp-12-829-2012)

1210 [Ng, N. L., Chhabra, P. S., Chan, A. W. H., Surratt, J. D., Kroll, J. H., Kwan, A. J., McCabe, D. C., Wennberg, P. O., Sorooshian, A., Murphy, S. M., Dalleska, N. F., Flagan, R. C., and Seinfeld, J. H.: Effect of NO<sub>x</sub> level on secondary organic aerosol \(SOA\) formation from the photooxidation of terpenes, Atmos Chem Phys, 7, 5159–5174, <https://doi.org/10.5194/acp-7-5159-2007>, 2007.](https://doi.org/10.1080/10618600.1999.10474853)

1215 [Paatero, P.: The Multilinear Engine—A Table-Driven, Least Squares Program for Solving Multilinear Problems, Including the n-Way Parallel Factor Analysis Model, Journal of Computational and Graphical Statistics, 8, 854–888, <https://doi.org/10.1080/10618600.1999.10474853>, 1999.](https://doi.org/10.1016/S0003-2670(02)01643-4)

1220 [Paatero, P. and Hopke, P. K.: Discarding or downweighting high-noise variables in factor analytic models, Anal Chim Acta, 490, 277–289, \[https://doi.org/10.1016/S0003-2670\\(02\\)01643-4\]\(https://doi.org/10.1016/S0003-2670\(02\)01643-4\), 2003.](https://doi.org/10.1016/S0003-2670(02)01643-4)

1225 [Paatero, P. and Tapper, U.: Analysis of different modes of factor analysis as least squares fit problems, Chemometrics and Intelligent Laboratory Systems, 18, 183–194, \[https://doi.org/10.1016/0169-7439\\(93\\)80055-M\]\(https://doi.org/10.1016/0169-7439\(93\)80055-M\), 1993.](https://doi.org/10.1016/0169-7439(93)80055-M)

1230 [Paatero, P. and Tapper, U.: Positive matrix factorization: A non-negative factor model with optimal utilization of error estimates of data values, Environmetrics, 5, 111–126, <https://doi.org/10.1002/env.3170050203>, 1994.](https://doi.org/10.1002/env.3170050203)

Paatero, P., Eberly, S., Brown, S. G., and Norris, G. A.: Methods for estimating uncertainty in factor analytic solutions, *Atmos Meas Tech*, 7, 781–797, <https://doi.org/10.5194/amt-7-781-2014>, 2014.

1220 Pallavi, Sinha, B., and Sinha, V.: Source apportionment of volatile organic compounds in the northwest Indo-Gangetic Plain using a positive matrix factorization model, *Atmos Chem Phys*, 19, 15467–15482, <https://doi.org/10.5194/acp-19-15467-2019>, 2019.

Pandey, P., Khan, A. H., Verma, A. K., Singh, K. A., Mathur, N., Kisku, G. C., and Barman, S. C.: Seasonal trends of PM 2.5 and PM 10 in ambient air and their correlation in ambient air of Lucknow City, India, *Bull Environ Contam Toxicol*, 88, 265–270, <https://doi.org/10.1007/s00128-011-0466-x>, 2012.

1225 Pandey, P., Patel, D. K., Khan, A. H., Barman, S. C., Murthy, R. C., and Kisku, G. C.: Temporal distribution of fine particulates (PM 2.5, PM 10), potentially toxic metals, PAHs and Metal-bound carcinogenic risk in the population of Lucknow City, India, *J Environ Sci Health A Tox Hazard Subst Environ Eng*, 48, 730–745, <https://doi.org/10.1080/10934529.2013.744613>, 2013.

1230 Petit, J. E., Favez, O., Albinet, A., and Canonaco, F.: A user-friendly tool for comprehensive evaluation of the geographical origins of atmospheric pollution: Wind and trajectory analyses, *Environmental Modelling and Software*, 88, 183–187, <https://doi.org/10.1016/j.envsoft.2016.11.022>, 2017.

Preuss, R., Angerer, J., and Drexler, H.: Naphthalene - An environmental and occupational toxicant, *Int Arch Occup Environ Health*, 76, 556–576, <https://doi.org/10.1007/s00420-003-0458-1>, 2003.

1235 Pye, H. O. T., Ward-Caviness, C. K., Murphy, B. N., Appel, K. W., and Seltzer, K. M.: Secondary organic aerosol association with cardiopulmonary disease mortality in the United States, *Nat Commun*, 12, 1–8, <https://doi.org/10.1038/s41467-021-27484-1>, 2021.

Qin, J., Wang, X., Yang, Y., Qin, Y., Shi, S., Xu, P., Chen, R., Zhou, X., Tan, J., and Wang, X.: Source apportionment of VOCs in a typical medium-sized city in North China Plain and implications on control policy, *Journal of Environmental Sciences*, 107, 26–37, <https://doi.org/10.1016/j.jes.2020.10.005>, 2021a.

1240 Qin, M., Murphy, B. N., Isaacs, K. K., McDonald, B. C., Lu, Q., McKeen, S. A., Koval, L., Robinson, A. L., Efthathiou, C., Allen, C., and Pye, H. O. T.: Criteria pollutant impacts of volatile chemical products informed by near-field modelling, *Nat Sustain*, 4, 129–137, <https://doi.org/10.1038/s41893-020-00614-1>, 2021b.

Sahu, L. K. and Saxena, P.: High time and mass resolved PTR-TOF-MS measurements of VOCs at an urban site of India during winter: Role of anthropogenic, biomass burning, biogenic and photochemical sources, *Atmos Res*, 164–165, 84–94, <https://doi.org/10.1016/j.atmosres.2015.04.021>, 2015.

1245 Sahu, L. K., Yadav, R., and Pal, D.: Source identification of VOCs at an urban site of western India: Effect of marathon events and anthropogenic emissions, *Journal of Geophysical Research: Atmospheres RESEARCH*, 121, 2416–2433, <https://doi.org/10.1002/2015JD024454>, 2016.

Sahu, L. K., Tripathi, N., and Yadav, R.: Contribution of biogenic and photochemical sources to ambient VOCs during winter to summer transition at a semi-arid urban site in India, *Environmental Pollution*, 229, 595–606, <https://doi.org/10.1016/j.envpol.2017.06.091>, 2017.

1250 Sandradewi, J., Prévôt, A. S. H., Szidat, S., Perron, N., Alfarra, M. R., Lanz, V. A., Weingartner, E., and Baltensperger, U. R. S.: Using aerosol light absorption measurements for the quantitative determination of wood burning and traffic emission contribution to particulate matter, *Environ Sci Technol*, 42, 3316–3323, <https://doi.org/10.1021/es702253m>, 2008.

1255 Sarkar, C., Sinha, V., Sinha, B., Panday, A. K., Rupakheti, M., and Lawrence, M. G.: Source apportionment of NMVOCs in the Kathmandu Valley during the SusKat-ABC international field campaign using positive matrix factorization, *Atmos Chem Phys*, 17, 8129–8156, <https://doi.org/10.5194/acp-17-8129-2017>, 2017.

Seco, R., Peñuelas, J., and Filella, I.: Short-chain oxygenated VOCs: Emission and uptake by plants and atmospheric sources, sinks, and concentrations, *Atmos Environ*, 41, 2477–2499, <https://doi.org/10.1016/j.atmosenv.2006.11.029>, 2007.

1260

Sekimoto, K., Koss, A. R., Gilman, J. B., Selimovic, V., Coggon, M. M., Zarzana, K. J., Yuan, B., Lerner, B. M., Brown, S. S., Warneke, C., Yokelson, R. J., Roberts, J. M., and De Gouw, J.: High-and low-temperature pyrolysis profiles describe volatile organic compound emissions from western US wildfire fuels, *Atmos Chem Phys*, 18, 9263–9281, <https://doi.org/10.5194/acp-18-9263-2018>, 2018.

1265 Sharma, K., Singh, R., Barman, S. C., Mishra, D., Kumar, R., Negi, M. P. S., Mandal, S. K., Kisku, G. C., Khan, A. H., Kidwai, M. M., and Bhargava, S. K.: Comparison of trace metals concentration in PM10 of different locations of Lucknow City, India, *Bull Environ Contam Toxicol*, 77, 419–426, <https://doi.org/10.1007/s00128-006-1082-z>, 2006.

1270 Sharma, S. and Khare, M.: Simulating ozone concentrations using precursor emission inventories in Delhi – National Capital Region of India, *Atmos Environ*, 151, 117–132, <https://doi.org/10.1016/j.atmosenv.2016.12.009>, 2017.

1275 Shukla, A. K., Lalchandani, V., Bhattu, D., Dave, J. S., Rai, P., Thamban, N. M., Mishra, S., Gaddamidi, S., Tripathi, N., Vats, P., Rastogi, N., Sahu, L., Ganguly, D., Kumar, M., Singh, V., Gargava, P., and Tripathi, S. N.: Real-time quantification and source apportionment of fine particulate matter including organics and elements in Delhi during summertime, *Atmos Environ*, 261, <https://doi.org/10.1016/j.atmosenv.2021.118598>, 2021.

1280 Simonelt, B. R. T., Rogge, W. F., Mazurek, M. A., Standley, L. J., Hildemann, L. M., and Cass, G. R.: Lignin Pyrolysis Products, Lignans, and Resin Acids as Specific Tracers of Plant Classes in Emissions from Biomass Combustion, *Environ Sci Technol*, 27, 2533–2541, <https://doi.org/10.1021/es00048a034>, 1993.

1285 Sinha, V., Kumar, V., and Sarkar, C.: Chemical composition of pre-monsoon air in the Indo-Gangetic Plain measured using a new air quality facility and PTR-MS: High surface ozone and strong influence of biomass burning, *Atmos Chem Phys*, 14, 5921–5941, <https://doi.org/10.5194/acp-14-5921-2014>, 2014.

1290 Smith, D. and Spanel, P.: Selected ion flow tube mass spectrometry SIFT-MS for on-line trace gas analysis, *Mass Spectrom Rev*, 24, 661–700, <https://doi.org/10.1002/mas.20033>, 2005.

1295 Sotiropoulou, R. E. P., Tagaris, E., Pilinis, C., Anttila, T., and Kulmala, M.: Modeling new particle formation during air pollution episodes: Impacts on aerosol and cloud condensation nuclei, *Aerosol Science and Technology*, 40, 557–572, <https://doi.org/10.1080/02786820600714346>, 2006.

1300 Srivastava, A., Sengupta, B., and Dutta, S. A.: Source apportionment of ambient VOCs in Delhi City, *Science of the Total Environment*, 343, 207–220, <https://doi.org/10.1016/j.scitotenv.2004.10.008>, 2005.

1305 Srivastava, A., Joseph, A. E., and Devotta, S.: Volatile organic compounds in ambient air of Mumbai - India, *Atmos Environ*, 40, 892–903, <https://doi.org/10.1016/j.atmosenv.2005.10.045>, 2006.

Steinbacher, M., Dommen, J., Ammann, C., Spirig, C., Neftel, A., and Prevot, A. S. H.: Performance characteristics of a proton-transfer-reaction mass spectrometer (PTR-MS) derived from laboratory and field measurements, *Int J Mass Spectrom*, 239, 117–128, <https://doi.org/10.1016/j.ijms.2004.07.015>, 2004.

Stewart, G. J., Nelson, B. S., Acton, W. J. F., Vaughan, A. R., Farren, N. J., Hopkins, J. R., Ward, M. W., Swift, S. J., Arya, R., Mondal, A., Jangirh, R., Ahlawat, S., Yadav, L., Sharma, S. K., Yunus, S. S. M., Nicholas Hewitt, C., Nemitz, E., Mullinger, N., Gadi, R., Sahu, L. K., Tripathi, N., Rickard, A. R., Lee, J. D., Mandal, T. K., and Hamilton, J. F.: Emissions of intermediate-volatility and semi-volatile organic compounds from combustion of domestic fuels in Delhi, India, *Atmos Chem Phys*, 21, 2407–2426, <https://doi.org/10.5194/acp-21-2383-2021>, 2021a.

Stewart, G. J., Acton, W. J. F., Nelson, B. S., Vaughan, A. R., Hopkins, J. R., Arya, R., Mondal, A., Jangirh, R., Ahlawat, S., Yadav, L., Sharma, S. K., Dunmore, R. E., Yunus, S. S. M., Nicholas Hewitt, C., Nemitz, E., Mullinger, N., Gadi, R., Sahu, L. K., Tripathi, N., Rickard, A. R., Lee, J. D., Mandal, T. K., and Hamilton, J. F.: Emissions of non-methane volatile organic compounds from combustion of domestic fuels in Delhi, India, *Atmos Chem Phys*, 21, 2383–2406, <https://doi.org/10.5194/acp-21-2383-2021>, 2021b.

Stewart, G. J., Nelson, B. S., Drysdale, W. S., Acton, W. J. F., Vaughan, A. R., Hopkins, J. R., Dunmore, R. E., Hewitt, C. N., Nemitz, E., Mullinger, N., Langford, B., Shivani, Reyes-Villegas, E., Gadi, R., Rickard, A. R., Lee,

J. D., and Hamilton, J. F.: Sources of non-methane hydrocarbons in surface air in Delhi, India, *Faraday Discuss.*, 226, 409–431, <https://doi.org/10.1039/d0fd00087f>, 2021c.

1310 Stockwell, C. E., Veres, P. R., Williams, J., and Yokelson, R. J.: Characterization of biomass burning emissions from cooking fires, peat, crop residue, and other fuels with high-resolution proton-transfer-reaction time-of-flight mass spectrometry, *Atmos Chem Phys.*, 15, 845–865, <https://doi.org/10.5194/acp-15-845-2015>, 2015.

Talukdar, S., Tripathi, S. N., Lalchandani, V., Rupakheti, M., Bhowmik, H. S., Shukla, A. K., Murari, V., Sahu, R., Jain, V., Tripathi, N., Dave, J., Rastogi, N., and Sahu, L.: Air pollution in new delhi during late winter: An overview of a group of campaign studies focusing on composition and sources, *Atmosphere (Basel)*, 12, 1–22, <https://doi.org/10.3390/atmos12111432>, 2021.

1315 Tan, Y., Han, S., Chen, Y., Zhang, Z., Li, H., Li, W., Yuan, Q., Li, X., Wang, T., and Lee, S. cheng: Characteristics and source apportionment of volatile organic compounds (VOCs) at a coastal site in Hong Kong, *Science of the Total Environment*, 777, 146241, <https://doi.org/10.1016/j.scitotenv.2021.146241>, 2021.

1320 Tang, T., Cheng, Z., Xu, B., Zhang, B., Zhu, S., Cheng, H., Li, J., Chen, Y., and Zhang, G.: Triple Isotopes ( $\delta^{13}\text{C}$ ,  $\delta^{2}\text{H}$ , and  $\Delta^{14}\text{C}$ ) Compositions and Source Apportionment of Atmospheric Naphthalene: A Key Surrogate of Intermediate-Volatility Organic Compounds (IVOCs), *Environ Sci Technol.*, 54, 5409–5418, <https://doi.org/10.1021/acs.est.0c00075>, 2020.

1325 Tobler, A., Bhattu, D., Canonaco, F., Lalchandani, V., Shukla, A., Thamban, N. M., Mishra, S., Srivastava, A. K., Bisht, D. S., Tiwari, S., Singh, S., Močnik, G., Baltensperger, U., Tripathi, S. N., Slowik, J. G., and Prévôt, A. S. H.: Chemical characterization of PM<sub>2.5</sub> and source apportionment of organic aerosol in New Delhi, India, *Science of the Total Environment*, 745, 1–12, <https://doi.org/10.1016/j.scitotenv.2020.140924>, 2020.

Tripathi, N. and Sahu, L.: Chemosphere Emissions and atmospheric concentrations of a -pinene at an urban site of India: Role of changes in meteorology, *Chemosphere*, 256, 127071, <https://doi.org/10.1016/j.chemosphere.2020.127071>, 2020.

1330 Tripathi, N., Sahu, L. K., Patel, K., Kumar, A., and Yadav, R.: Ambient air characteristics of biogenic volatile organic compounds at a tropical evergreen forest site in Central Western Ghats of India, *J Atmos Chem*, 78, 139–159, <https://doi.org/10.1007/s10874-021-09415-y>, 2021.

1335 Tripathi, N., Sahu, L. K., Wang, L., Vats, P., Soni, M., Kumar, P., Satis, R. V., Bhattu, D., Sahu, R., Patel, K., Rai, P., Kumar, V., Rastogi, N., Ojha, N., Tiwari, S., Ganguly, D., Slowik, J., Prévôt, A. S. H., and Tripathi, S. N.: Characteristics of VOC composition at urban and suburban sites of New Delhi, India in winter, *Journal of Geophysical Research: Atmospheres*, 1–28, <https://doi.org/10.1029/2021jd035342>, 2022.

Ulbrich, I. M., Canagaratna, M. R., Zhang, Q., Worsnop, D. R., and Jimenez, J. L.: Interpretation of organic components from Positive Matrix Factorization of aerosol mass spectrometric data, *Atmos Chem Phys.*, 9, 2891–2918, <https://doi.org/10.5194/acp-9-2891-2009>, 2009.

1340 Uttar Pradesh Pollution Control Board: Action Plan for the control of Air Pollution in Lucknow city, 2019.

Wang, G., Cheng, S., Wei, W., Zhou, Y., Yao, S., and Zhang, H.: Characteristics and source apportionment of VOCs in the suburban area of Beijing, China, *Atmos Pollut Res.*, 7, 711–724, <https://doi.org/10.1016/j.apr.2016.03.006>, 2016.

1345 Wang, L., Slowik, J., Tripathi, N., Bhattu, D., Rai, P., Kumar, V., Vats, P., Satis, R., Baltensperger, U., Ganguly, D., Rastogi, N., Sahu, L., Tripathi, S., and Prévôt, A.: Source characterization of volatile organic compounds measured by PTR-ToF-MS in Delhi, India, *Atmos Chem Phys.*, 1–27, <https://doi.org/10.5194/acp-2020-11>, 2020a.

Wang, L., Slowik, J. G., Tong, Y., Duan, J., Gu, Y., Rai, P., Qi, L., Stefenelli, G., Baltensperger, U., Huang, R. J., Cao, J., and Prévôt, A. S. H.: Characteristics of wintertime VOCs in urban Beijing: Composition and source apportionment, *Atmos Environ X*, 9, <https://doi.org/10.1016/j.aeaoa.2020.100100>, 2021a.

1350 Wang, S., Newland, M. J., Deng, W., Rickard, A. R., Hamilton, J. F., Muñoz, A., Ródenas, M., Vázquez, M. M., Wang, L., and Wang, X.: Aromatic Photo-oxidation, A New Source of Atmospheric Acidity, *Environ Sci Technol.*, 54, 7798–7806, <https://doi.org/10.1021/acs.est.0c00526>, 2020b.

1355 Wang, S. X., Zhao, B., Cai, S. Y., Klimont, Z., Nielsen, C. P., Morikawa, T., Woo, J. H., Kim, Y., Fu, X., Xu, J., Y., Hao, J. M., and He, K. B.: Emission trends and mitigation options for air pollutants in East Asia, *Atmos Chem Phys*, 14, 6571–6603, <https://doi.org/10.5194/acp-14-6571-2014>, 2014.

1360 Warneke, C., de Gouw, J. A., Goldan, P. D., Kuster, W. C., Williams, E. J., Lerner, B. M., Jakoubek, R., Brown, S. S., Stark, H., Aldener, M., Ravishankara, A. R., Roberts, J. M., Marchewka, M., Bertman, S., Sueper, D. T., McKeen, S. A., Meagher, J. F., and Fehsenfeld, F. C.: Comparison of daytime and nighttime oxidation of biogenic and anthropogenic VOCs along the New England coast in summer during New England Air Quality Study 2002, *Journal of Geophysical Research D: Atmospheres*, 109, 1–14, <https://doi.org/10.1029/2003JD004424>, 2004.

1365 WHO: IARC Monographs on the identification of carcinogenic hazards to Humans, 2021.

1370 Wu, J., Kong, S., Wu, F., Cheng, Y., Zheng, S., Qin, S., Liu, X., Yan, Q., Zheng, H., Zheng, M., Yan, Y., Liu, D., Ding, S., Zhao, D., Shen, G., Zhao, T., and Qi, S.: The moving of high emission for biomass burning in China: View from multi-year emission estimation and human-driven forces, *Environ Int*, 142, 105812, <https://doi.org/10.1016/j.envint.2020.105812>, 2020.

1375 Xu, L., Kollman, M. S., Song, C., Shilling, J. E., and Ng, N. L.: Effects of NO<sub>x</sub> on the Volatility of Secondary Organic Aerosol from Isoprene Photooxidation, *Environ Sci Technol*, 48, 2253–2262, <https://doi.org/https://doi.org/10.1021/es404842g>, 2014.

1380 Yadav, M., Soni, K., Soni, B. K., Singh, N. K., and Bamniya, B. R.: Source apportionment of particulate matter, gaseous pollutants, and volatile organic compounds in a future smart city of India, *Urban Clim*, 28, 100470, <https://doi.org/10.1016/j.uclim.2019.100470>, 2019.

1385 Yang, W., Zhang, Y., Wang, X., Li, S., Zhu, M., Yu, Q., Li, G., Huang, Z., Zhang, H., Wu, Z., Song, W., Tan, J., and Shao, M.: Volatile organic compounds at a rural site in Beijing: Influence of temporary emission control and wintertime heating, *Atmos Chem Phys*, 18, 12663–12682, <https://doi.org/10.5194/acp-18-12663-2018>, 2018.

1390 Yee, L. D., Kautzman, K. E., Loza, C. L., Schilling, K. A., Coggon, M. M., Chhabra, P. S., Chan, M. N., Chan, A. W. H., Hersey, S. P., Crounse, J. D., Wennberg, P. O., Flagan, R. C., and Seinfeld, J. H.: Secondary organic aerosol formation from biomass burning intermediates: Phenol and methoxyphenols, *Atmos Chem Phys*, 13, 8019–8043, <https://doi.org/10.5194/acp-13-8019-2013>, 2013.

1395 Zhan, J., Feng, Z., Liu, P., He, X., He, Z., Chen, T., Wang, Y., He, H., Mu, Y., and Liu, Y.: Ozone and SOA formation potential based on photochemical loss of VOCs during the Beijing summer, *Environmental Pollution*, 285, 117444, <https://doi.org/10.1016/j.envpol.2021.117444>, 2021.

1400 Zhang, F., Xing, J., Zhou, Y., Wang, S., Zhao, B., Zheng, H., Zhao, X., Chang, H., Jang, C., Zhu, Y., and Hao, J.: Estimation of abatement potentials and costs of air pollution emissions in China, *J Environ Manage*, 260, 110069, <https://doi.org/10.1016/j.jenvman.2020.110069>, 2020.

1405 Zhang, Q., Jimenez, J. L., Canagaratna, M. R., Ulbrich, I. M., Ng, N. L., Worsnop, D. R., and Sun, Y.: Understanding atmospheric organic aerosols via factor analysis of aerosol mass spectrometry: A review, *Anal Bioanal Chem*, 401, 3045–3067, <https://doi.org/10.1007/s00216-011-5355-y>, 2011.

1410 Zhang, Z., Wang, H., Chen, D., Li, Q., Thai, P., Gong, D., Li, Y., Zhang, C., Gu, Y., Zhou, L., Morawska, L., and Wang, B.: Emission characteristics of volatile organic compounds and their secondary organic aerosol formation potentials from a petroleum refinery in Pearl River Delta, China, *Science of the Total Environment*, 584–585, 1162–1174, <https://doi.org/10.1016/j.scitotenv.2017.01.179>, 2017.

1415 Zheng, J., Shao, M., Che, W., Zhang, L., Zhong, L., Zhang, Y., and Streets, D.: Speciated VOC emission inventory and spatial patterns of ozone formation potential in the Pearl River Delta, China, *Environ Sci Technol*, 43, 8580–8586, <https://doi.org/10.1021/es901688e>, 2009.

1420 Zhu, Y., Yang, L., Chen, J., Wang, X., Xue, L., Sui, X., Wen, L., Xu, C., Yao, L., Zhang, J., Shao, M., Lu, S., and Wang, W.: Characteristics of ambient volatile organic compounds and the influence of biomass burning at a rural site in Northern China during summer 2013, *Atmos Environ*, 124, 156–165, <https://doi.org/10.1016/j.atmosenv.2015.08.097>, 2016.

1400

Zotter, P., Herich, H., Gysel, M., El-Haddad, I., Zhang, Y., Mocnik, G., Hüglin, C., Baltensperger, U., Szidat, S., and Prévôt, A. S. H.: Evaluation of the absorption Ångström exponents for traffic and wood burning in the Aethalometer-based source apportionment using radiocarbon measurements of ambient aerosol, Atmos Chem Phys, 17, 4229–4249, <https://doi.org/10.5194/acp-17-4229-2017>, 2017.

1405

1410

1415

1420

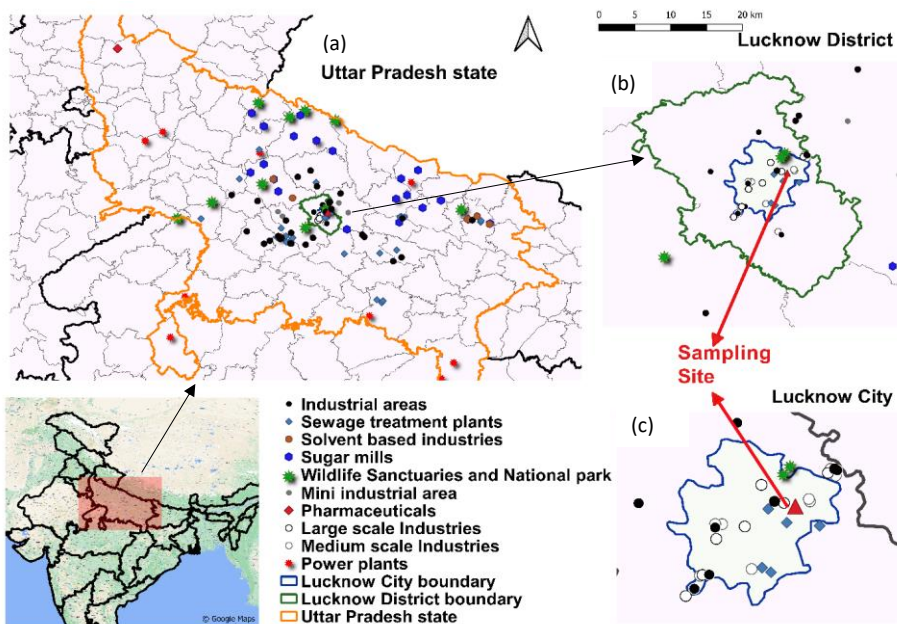


Figure 1: Detailed map of (a) Uttar Pradesh, (b) Lucknow district and (c) Lucknow City with highlighted sampling site and major potential point-sources of NMVOCs

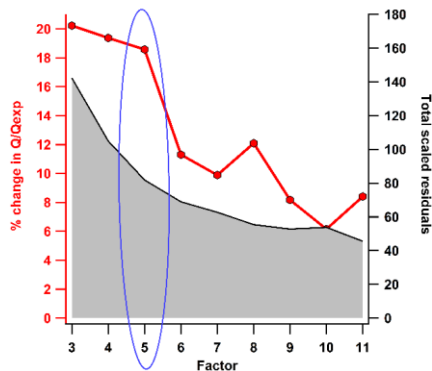


Figure 2: The Q/Qexp plot (% change) and total summed scaled residuals for each factor solution

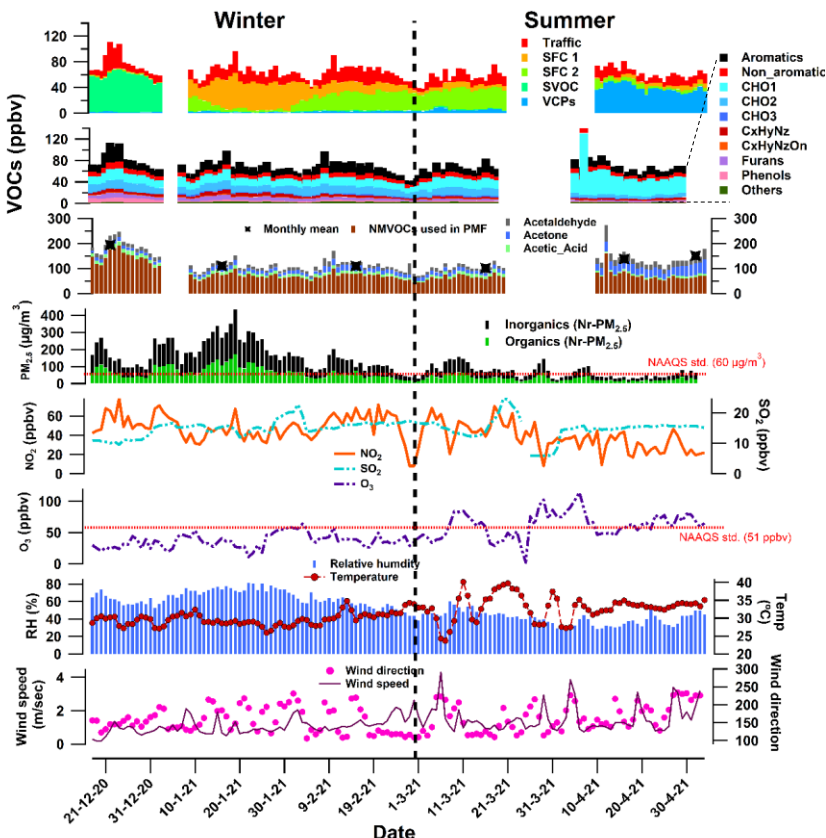


Figure 3: Daily averaged time series of acetaldehyde, acetone, and acetic acid, other NMVOCs, PM<sub>2.5</sub> and its organic fraction, NO<sub>2</sub>, SO<sub>2</sub>, O<sub>3</sub>, temperature, relative humidity, and wind speed and direction

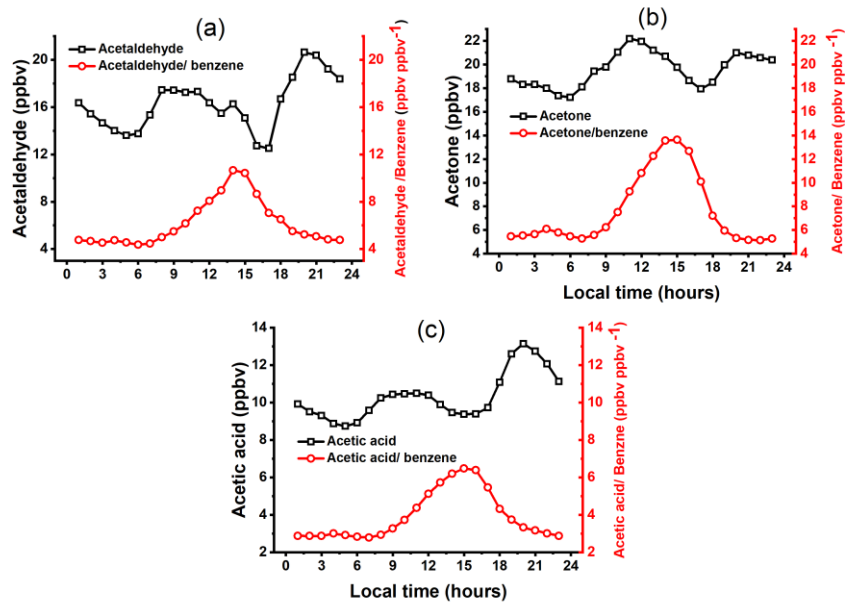
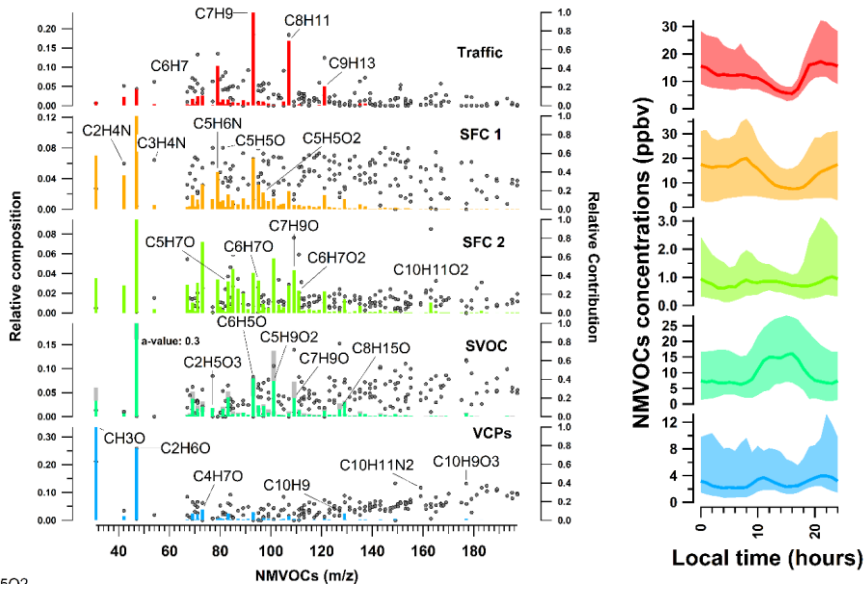


Figure 4: Diurnal variations over the whole study period for (a) Acetaldehyde and Acetaldehyde/benzene ratio, (b) Acetone and Acetone/benzene ratio, and (c) Acetic acid and Acetic acid/benzene ratio

1465

1470

1475



**Figure 5: Profile and diurnal variation of individual factors of selected 5-factor solution after PMF analysis at Lucknow for the whole study period. In (a), the left axis represents the relative composition of each factor, given by the vertical bars. The sum of all the bars at different  $m/z$  for each factor is 1, and the right axis represents the relative contribution of each factor to a given  $m/z$ , shown as grey dots. The grey bars in the SVOC factor represents the degree of constraint on the known source profile and time series. In (b) the middle dark line represents the median of the diurnal while the shaded region represents the interquartile ranges from 25-75<sup>th</sup> percentiles.**

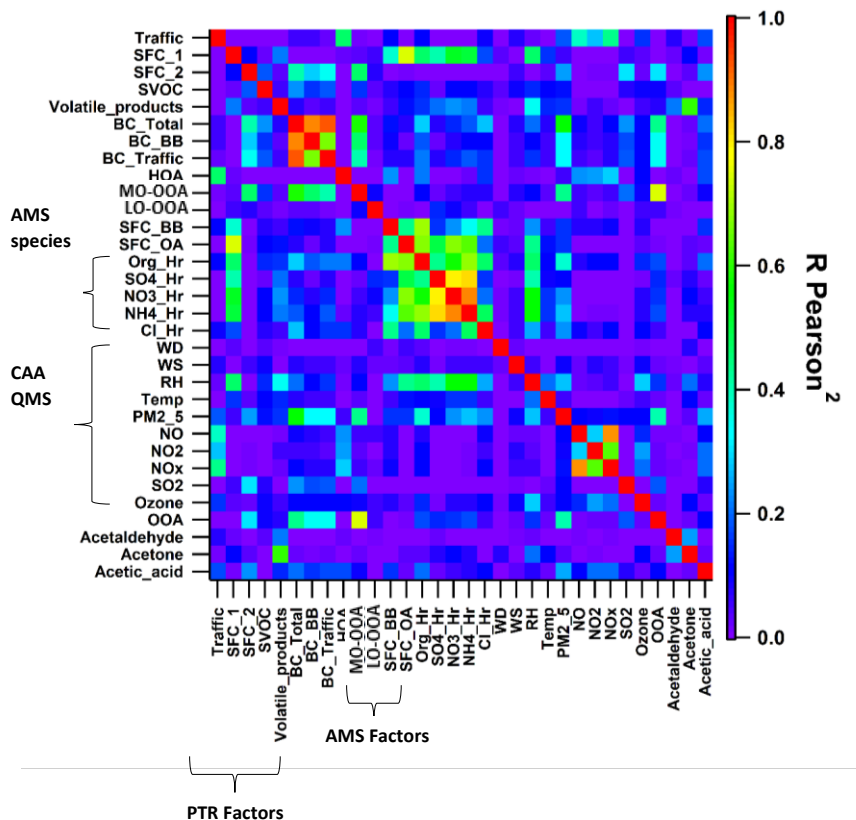


Figure 6: Correlation of the five factors to the external measurements, including factors from AMS, Organics NR-PM<sub>2.5</sub> and Inorganics NR-PM<sub>2.5</sub>, Black carbon (BC total, % BC from fossil and non-fossil fuels), CAAQMS data, total oxygenated organic aerosols (OOA), VOCs species. The CAAQMS data includes wind direction (WD), wind speed (WS), relative humidity (RH), ambient temperature (Temp), Particulate matter (PM2.5), nitric oxide (NO), nitrogen dioxide (NO<sub>2</sub>), nitrogen oxides (NOx), sulphur dioxide (SO<sub>2</sub>) and Ozone. The correlation between the timeseries of the parameters is represented by R Pearson<sup>2</sup>, colour coded with rainbow color scheme, showing violet as 0 (no correlation) and red as 1 (highest correlation).

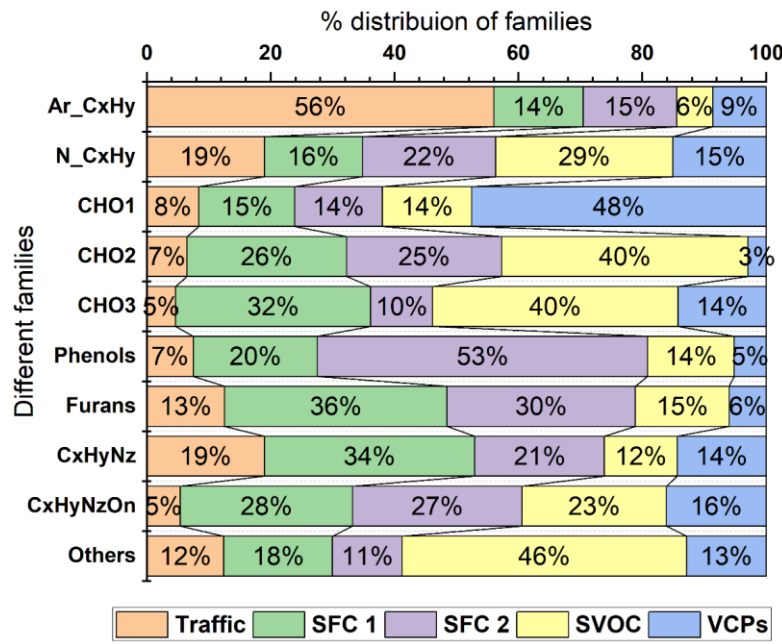


Figure 7: Relative contributions (%) of different families to the individual factors

1495

1500

1505

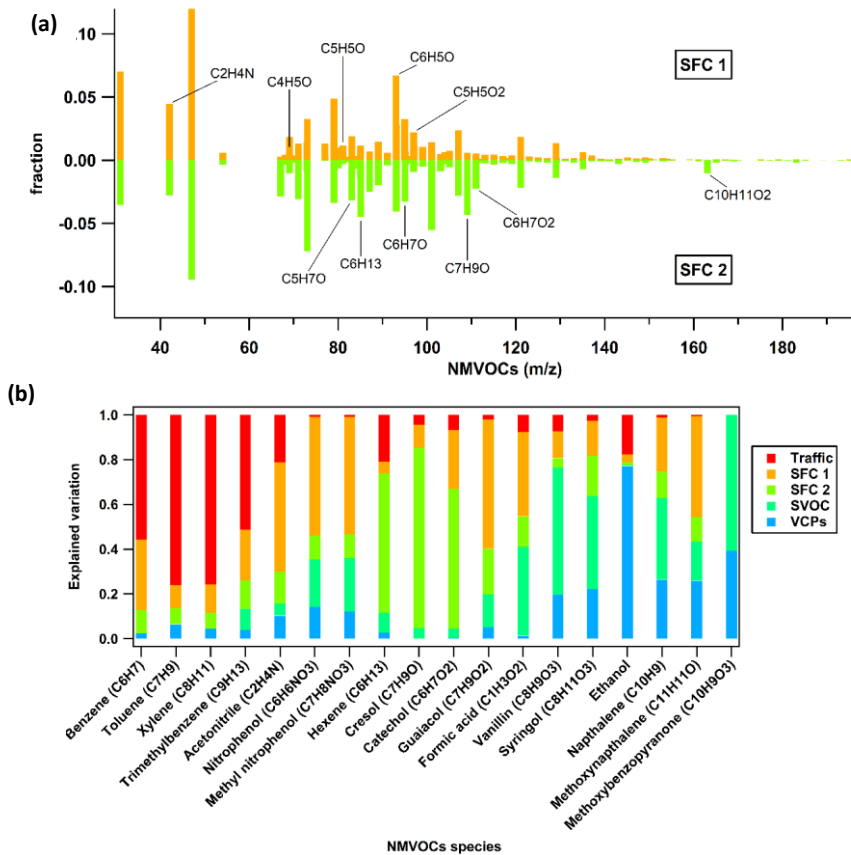
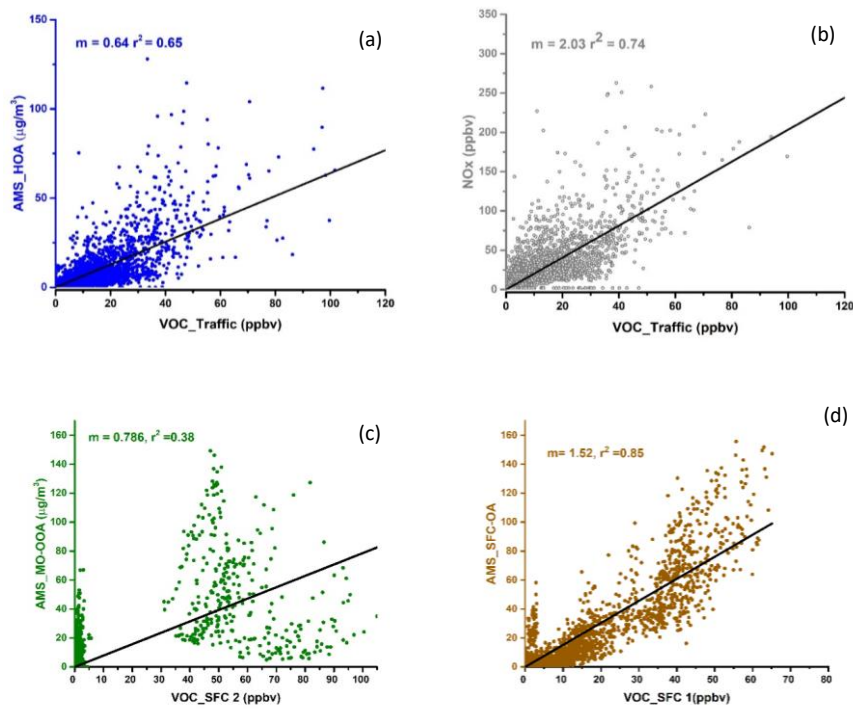
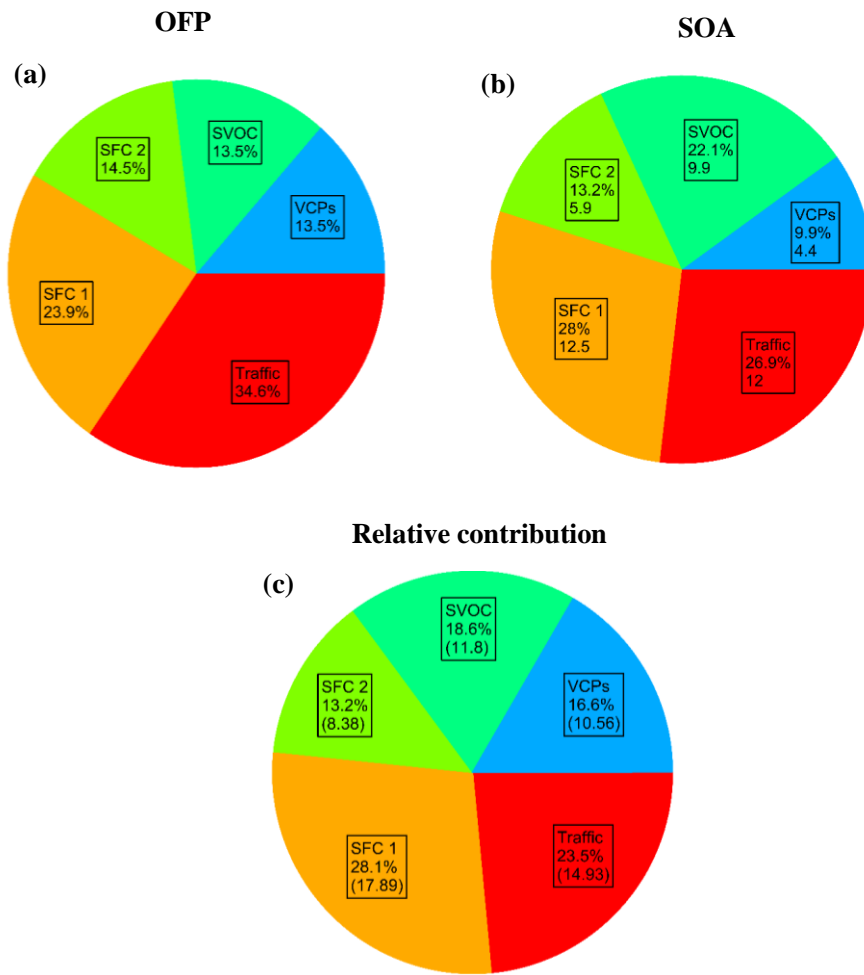


Figure 8: (a) Comparison of relative composition of two factor profiles (SFC 1 and SFC 2). SFC 1 spectrum on top and SFC 2 spectrum on bottom. (b) Explained variation of selected NMVOCs species, stacked such that total explained variation is 1, colour coded by the five factors.



[Figure 9: Scatter plots showing a correlation between VOC factors with their respective AMS factors](#)



**Figure 10:** Distribution in percentage (%) of individual factors to (a) Ozone formation potential (OFP), (b) SOA formation, (c) Relative contribution. The bottom absolute values (in brackets) for (b) and (c) are the SOA yield mass concentration ( $\mu\text{g}/\text{m}^3$ ) and average mixing ratios (ppbv)

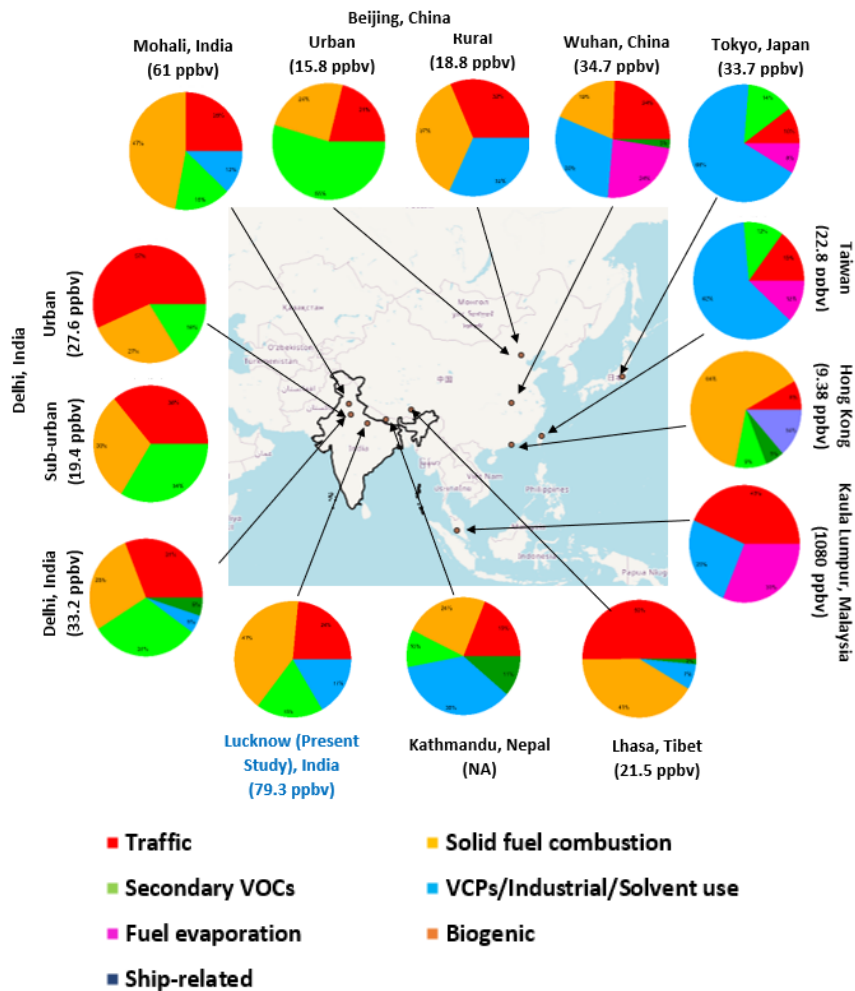


Figure 11: Mapped- Pie charts showing various sources of NMVOCs in different Asian and Indian cities. The bottom values (in brackets) represent the averaged mixing ratios of total NMVOCs in respective study.

Formatted: Indent: Left: 0 cm, First line: 0 cm, Line spacing: Multiple 1.08 li, Widow/Orphan control, Suppress line numbers, Adjust space between Latin and Asian text, Adjust space between Asian text and numbers